



HAL
open science

Lymphocytes perform reverse adhesive haptotaxis mediated by LFA-1 integrins

Xuan Luo, Valentine Seveau de Noray, Laurene Aoun, Martine Biarnes-Pelicot, Pierre-Olivier Strale, Vincent Studer, Marie-Pierre Valignat, Olivier Théodoly

► To cite this version:

Xuan Luo, Valentine Seveau de Noray, Laurene Aoun, Martine Biarnes-Pelicot, Pierre-Olivier Strale, et al.. Lymphocytes perform reverse adhesive haptotaxis mediated by LFA-1 integrins. *Journal of Cell Science*, 2020, 133 (16), pp.jcs242883. 10.1242/jcs.242883 . hal-03006730

HAL Id: hal-03006730

<https://hal.science/hal-03006730>

Submitted on 17 Dec 2020

HAL is a multi-disciplinary open access archive for the deposit and dissemination of scientific research documents, whether they are published or not. The documents may come from teaching and research institutions in France or abroad, or from public or private research centers.

L'archive ouverte pluridisciplinaire **HAL**, est destinée au dépôt et à la diffusion de documents scientifiques de niveau recherche, publiés ou non, émanant des établissements d'enseignement et de recherche français ou étrangers, des laboratoires publics ou privés.

Lymphocyte perform reverse adhesive haptotaxis mediated by integrins LFA-1

Xuan Luo¹, Valentine Seveau de Noray¹, Laurene Aoun¹, Martine Biarnes-Pelicot¹, Pierre-Olivier Strale⁴, Vincent Studer^{2,3}, Marie-Pierre Valignat¹, Olivier Theodoly^{1,*}

¹ LAI, Aix Marseille Univ, CNRS, INSERM, Marseille, France.

² University of Bordeaux, Interdisciplinary Institute for Neuroscience, Bordeaux, France.

³ CNRS UMR 5297, F-33000 Bordeaux, France.

⁴ ALVEOLE, Paris, France

*Corresponding author.

Running title: *Reverse adhesive haptotaxis*

Summary statement: *Like mesenchymal cells, lymphocytes perform adhesive haptotaxis although adhesion is dispensable for amoeboid migration. Moreover, unlike mesenchymal cells, lymphocytes display a unique ability to follow decreasing gradients of adhesion.*

Keywords: haptotaxis, cell guidance, amoeboid migration, lymphocyte, integrins, LFA-1

ABSTRACT

Cell Guidance by anchored molecules, or haptotaxis, is crucial in development, immunology and cancer. Adhesive haptotaxis, or guidance by adhesion molecules, is well established for mesenchymal cells like fibroblasts, whereas its existence remains unreported for amoeboid cells that require less or no adhesion to migrate. We show here *in vitro* that amoeboid human T lymphocytes develop adhesive haptotaxis versus densities of integrin ligands expressed by high endothelial venules. Moreover, lymphocytes orient towards increasing adhesion with VLA-4 integrins, like all mesenchymal cells, but towards decreasing adhesion with LFA-1 integrins, which has never been observed. This counterintuitive ‘reverse haptotaxis’ cannot be explained with the existing mesenchymal mechanisms of competition between cells’ pulling edges or of lamellipodia growth activated by integrins, which favor orientation towards increasing adhesion. Mechanisms and functions of amoeboid adhesive haptotaxis remain unclear, however multidirectional integrin-mediated haptotaxis may operate around transmigration ports on endothelium, stromal cells in lymph nodes, and inflamed tissue where integrin ligands are spatially modulated.

INTRODUCTION

An efficient immune response requires the rapid recruitment of circulating leukocytes from the blood system to lymph nodes and inflamed tissues. Leukocytes arrest on the endothelium of blood vessels - the cellular monolayer covering the lumen -, then migrate spontaneously with a rapid 'crawling' mode, and eventually cross the endothelium - an event called diapedesis. On blood vessels walls, leukocytes crawl distances of several tens or hundreds of micrometers, proposedly in search for optimal diapedesis sites (Massena and Phillipson, 2012; Sumagin and Sarelius, 2010; Sumagin et al., 2010) called "transmigratory cups"(Carman and Springer, 2004) or "portals"(Sumagin and Sarelius, 2010). These sites are composed of endothelial cells with vertical microvilli-like projections enriched in adhesion molecules, notably the integrin ligands ICAM-1 (intercellular adhesion molecule-1) and VCAM-1 (vascular cell adhesion molecule-1). ICAM-1 was found particularly important to favor transmigration in nearby portals(Park et al., 2010; Sumagin and Sarelius, 2010), suggesting that integrins may guide leukocytes towards and through extravasation sites. After diapedesis, leukocytes migrate in three-dimensional environments of tissues and organs, where integrins-mediated adhesion was shown to be dispensable for motility (5,6). Nevertheless, integrins remain crucial *in vivo* for efficient homing, and the microenvironment of inflamed tissues is known to enhance motility with an integrin-dependent manner (Hons et al., 2018; Lämmermann et al., 2013; Overstreet et al., 2013). An important role of integrins was further established in the context of tumors, like the chronic lymphocytic leukemia (CLL), where VLA-4 expression on CLL cells had prognostic impact by favoring B cell adhesion and proliferation on stromal cells(Burger et al., 2009; Gattei et al., 2008). Also, the traffic of lymphocytes in lymph nodes is orchestrated by specialized stromal cells expressing integrin ligands and chemokines, and it has been hypothesized that integrins participate to guiding lymphocytes on the stromal network (Bajénoff et al., 2006). Altogether, guided migration by integrins is potentially relevant in several steps of leukocytes survey functions, however there is no direct evidence yet that integrins can guide leukocytes in environments presenting modulation of adhesion ligands density. The first goal of this work is therefore to investigate the existence and conditions of emergence of integrins-mediated guidance with amoeboid cells like leukocytes.

Directed motion is a hallmark of the immune response and several guiding cues are well identified. Leukocytes are sensitive to mechanical cues like the blood flow (mechanotaxis)(Dominguez et al., 2015; Gorina et al., 2014; Valignat et al., 2013; Valignat et al., 2014), to soluble biochemical cues like bacterial fragments or chemokines (chemotaxis) (Liu et al., 2012; Malawista et al., 2000; Malet-Engra et al., 2015; Massena and Phillipson, 2012; Poznansky et al., 2000; Tharp et al., 2006), and to anchored signaling molecules like the chemokines CCL21 or IL8 (haptotaxis) (Canton, 2008; Roy et al., 2017; Schwarz et al., 2017; van Gils et al., 2013; Weber et al., 2013). Directed motion by adhesion molecules is documented for mesenchymal cells like cancer cells, fibroblasts, muscle cells, endothelial cells(King et al., 2016; MacNearney et al., 2016; Oudin et al., 2016; Wen et al., 2015; Wu et al., 2012) as well as for Schwann cells(Motta et al., 2019) and neurons (Aznavorian et al., 1990; Brandley and Schnaar, 1989; Carter, 1965; Carter, 1967; Klominek et al., 1993; Mccarthy and Furcht, 1984; O'Connor et al., 1990; Smith et al., 2004; Thibault et al., 2007), but it has not been evidenced yet for amoeboid cells in general and for leukocytes in particular. For clarity, we call thereafter 'haptotaxis' any guidance phenotype triggered by anchored molecules, and 'adhesive haptotaxis' the guidance phenotypes specifically triggered by adhesion molecules. For mesenchymal migration, adhesive haptotaxis was initially explained by a tug of war in the

cell adherence zone, the areas with lower grip destabilizing spontaneously under traction in favor of areas with a higher grip (Caballero et al., 2015; Carter, 1965; Carter, 1967; O'Connor et al., 1990). Mesenchymal cells are indeed characterized by strong cell/substrate adhesion mediated by mature focal adhesions and by strong traction forces transmitted to the substrate by contractile actin stress fibers. In contrast, amoeboid cells migrate at high speed with weak adhesion and low traction forces transferred to the substrate (Lämmermann et al., 2008a; Paluch et al., 2016; Ricoult et al., 2015; Smith et al., 2007). Leukocytes can even swim without interaction with a substrate (Aoun et al.). A tug of war mechanism, with an interplay of strong adhesion and high traction, is therefore irrelevant for amoeboid cells and the existence of adhesive haptotaxis is all but evident for leukocytes.

Adhesive haptotaxis may however rely on mechanisms more sophisticated than a tug of war, especially when integrins are involved (King et al., 2016). Integrins are indeed more than adhesion molecules, as they can transduce signal when they engage to their ligands and are submitted to a force - a phenomenon called mechanotransduction (Ross et al., 2013; Zaidel-Bar et al., 2005). Adhesive haptotaxis mediated by integrins can therefore involve signaling transducing by integrins relayed by internal signaling pathways to transform external cues into cytoskeleton reorganization, like in chemotaxis (Artemenko et al., 2016; Aznavoorian et al., 1990; Klominek et al., 1993; Malawista et al., 2000; Massena and Phillipson, 2012; Thibault et al., 2007). Fundamentally, different paradigms can therefore sustain integrin-mediated adhesive haptotaxis, either active mechanisms relying on mechanotransduction of integrins acting as mechanoreceptors, or passive mechanisms based on physical competition between cell edges attached with integrins acting as adhesion linkers only.

To scrutinize guided migration by integrins, we performed here quantitative *in vitro* experiments and took advantage of technological advances in surface patterning methods (Strale et al., 2016). Our aim was not to answer whether leukocytes were guided by adherent versus non-adherent substrates, but more specifically whether integrins could sense modulations of adhesion on a globally adherent substrate. This latter case of globally adherent substrates is indeed directly relevant for leukocytes crawling on blood vessels, where adhesion is required at all times to resist the shear stress of blood flow (Granger and Kubes, 1994), as well as in tissues around scars (Berry et al., 2006; Sullivan et al., 2014; Wen et al., 2015), and in lymphoid organs where cells are generally exposed to integrin ligands (Bajénoff et al., 2006). In all these cases, haptotaxis requires mechanosensibility to variable adhesion and cannot be attributed to a trivial migration bias by lack of adhesion. For this task, usual microcontact-printing techniques with stamps were not adapted because they produce substrates with binary patterns of adherent and non-adherent areas. In order to produce patterns with multiple levels of integrin-ligands on a glass substrate, we developed an original 'subtractive printing protocol' based on the light induced multiple adsorption setup (Strale et al., 2016). We focused our study on coatings of ICAM-1 or VCAM-1 proteins, respectively ligands of integrins LFA-1 ($\alpha_1\beta_2$) and VLA-4 ($\alpha_4\beta_1$), and studied effector human primary T lymphocytes. Our results demonstrate the existence of sensitive and versatile adhesive haptotaxis mediated by integrins towards increasing adhesion with VLA-4 and, quite counterintuitively, towards decreasing adhesion with LFA-1. Mechanisms proposed for mesenchymal haptotaxis cannot explain this latter 'reverse haptotaxis' phenotype and a novel mechanism remains to be deciphered.

RESULTS

Protein printing yields adherent substrates with modulated densities of integrin ligands

In order to pattern substrates with controlled amounts of adhesion molecules, we used a set-up of light induced molecular adsorption or LIMA (Strale et al., 2016), which optically coupled a 375 nm UV light source with a Digital Micro-mirror Device (DMD) on an inverted microscope (). A specific patterning protocol of 'subtractive printing' was developed here to engineer substrates with modulated and integrin-specific adherence for lymphocytes. Glass coverslips were first treated with aminopropyltriethoxysilane (APTES), then sequentially incubated with solutions of Protein A, Bovine serum albumin (BSA) and chimera Fc-ICAM-1 or Fc-VCAM-1 (Fig. 1B). UV illumination was then used to degrade the functionality of ICAM-1 or VCAM-1 in presence of the photo-activator. Degradation was UV-dose dependent and grey-leveled illumination allowed us to obtain substrates with gradual adhesion properties. Fig.1C shows an immunofluorescence microscopy image of an ICAM-1 printed substrate, illuminated with stripes of different UV doses. The maximum dose was of 800 mJ/mm² and the pattern of illumination corresponded to 9 stripes of doses ranging between 10, 20, 30, 40, 50, 60, 70, 80, 90 and 100% of the maximum dose intercalated with stripes without illumination (Fig. 1A). The different levels of fluorescence brightness in Fig. 1C,D correspond to different surface densities of functional protein A, that then lead to different adsorbed amounts of Fc-CAM adhesion molecules. The amount of grafted CAM molecules was further assessed by imaging substrates after incubation with specific antibodies against ICAM-1 and VCAM-1. A calibration procedure, based on microfluidic channels filled with known amounts of fluorescent molecules, allowed us to convert immunofluorescent data into densities of CAM molecules on the substrates (see details in material and methods). The accessible densities of ICAM-1 and VCAM-1 molecules ranged between 0 and roughly 1000 molecules.μm⁻² (Fig. 1D), which corresponds to physiological levels found on the walls of high endothelial venules (Dustin and Springer, 1988).

Cell adhesion is controlled by integrins ligands density

To quantify the adhesion strength of lymphocytes versus the densities of ICAM-1 and VCAM-1, homogeneous substrates with different levels of integrins ligands densities were prepared by applying different UV-doses. Cells were seeded for 10 min on each substrate and submitted to a gentle shear stress of 1 dyn.cm⁻² to wash out non-adherent cells. The adhesion strength was then assessed by the ratio between the number of cells still adherent after 5 min under a shear stress of 8 dyn.cm⁻² and the number of initially adherent cells after initial wash at 1 dyn.cm⁻² (Fig. 1E). This ratio is later called 'Adhesion Rate'.

$$\text{Eqn. 1} \quad \text{Adhesion rate} = \frac{\# \text{ adherent cells at } 8 \text{ dyn.cm}^{-2}}{\# \text{ adherent cells at } 0 \text{ dyn.cm}^{-2}}$$

For ICAM-1 and VCAM-1, the adhesion rate was null below densities of 150-200 molecules.μm⁻², and increased until a plateau at 0.6 for ligands densities around 1000 molecules.μm⁻² (Fig. 1-F,G). These data attest that ligand density variations allowed us to tune cell adhesion.

Crenel profiles of adhesion allow rapid screening of haptotaxis existence

Haptotaxis corresponds to cell guidance by gradients of surface concentration of a component, and a complete characterization of a haptotaxis phenotype requires to screen different parameters of the stimulus sensed by individual cells, namely the local concentration of component, and the steepness and the direction of the gradient of component. The determination of the existence of haptotaxis can however be screened with fewer variables by selecting the optimal conditions for its emergence. Optimal conditions require a maximal cue difference between cell rear and front, as well as cue levels that are not too low (i.e. below detection level) nor too high (above saturation level). We therefore prepared crenel profiles of adhesion with alternated stripes of two different adhesion rates, comprised between the minimal and maximal adhesion rates sustaining cell adhesion. These patterns yielded adhesion gradients of maximal steepness at the frontier of stripes. Furthermore, in order to optimize the occurrence of events of cells having to choose direction at frontiers between stripes, the width of the stripes was chosen at 20 μm , slightly larger than the average diameter of adherent cells of $15 \pm 2 \mu\text{m}$.

In a given assay, we defined the 'adhesion contrast' between stripes as the difference in percent between the adhesion rates of stripes normalized by the maximal adhesion rate (Eqn. 2).

$$\text{Eqn. 2} \quad \textit{Adhesion contrast} = \frac{\textit{High adhesion rate} - \textit{Low adhesion rate}}{\textit{High adhesion rate}} \cdot 100$$

For all assays, the adhesion rate of stripes with high adhesion was kept at the maximum value of 0.6, whereas the adhesion rate of the stripes with low adhesion was varied from one assay to the other between 0 and 0.6. The range of assays varied therefore from an adhesion contrast of 0%, which corresponded to a homogeneous substrate (with the maximal adhesion rate of 0.6), and an adhesion contrast of 100%, which corresponded to alternated stripes of maximal and null adhesion rates. Adhesion rates and CAM molecules densities were systematically measured in each experiment and for each stripe type. In the following, guidance properties are plotted versus substrates adhesion properties, and the correspondence between adhesion properties and ligand densities are accessible from Fig. 1G.

Direction of crawling lymphocytes is biased by non-adherent stripes

Cells trajectories were tracked for 16 min and the orientation of each individual cell was assessed from the orientation between first and final positions. Due to the symmetry of the assays, opposite directions are equivalent and a cell preference between stripes may yield an anisotropy in orientation but not a preferential direction, so that usual chemotactic (or haptotactic) index is also not adapted here. A preference between opposite direction could emerge from a chirality effect in the biological system but this is not related to the haptotactic prowess of interest here. Hence, to assess the existence of guidance in our assays, we defined an 'anisotropy index' to reveal and quantify a sensitivity of cells to modulations of substrate adhesion. Distribution of orientations were displayed on rose wind plots and the 'Anisotropy Index' was defined as the normalized difference between the cell fractions in vertical quadrants (orientation bias parallel to stripes) and in horizontal quadrants (orientation bias perpendicular to stripes) of the rose wind plot (Fig. 2 and Eqn. 3).

Eqn. 3 *Anisotropy index =*

$$\frac{\# \text{ cells oriented in vertical quadrants} - \# \text{ cells oriented in horizontal quadrants}}{\# \text{ cells total}}$$

Control experiments corresponded to substrates with homogeneous adhesion, i.e. to an adhesion contrast of 0%. The rose wind plots of direction were isotropic for these controls and the anisotropy index equal to 0 (Fig. 2A, and left panels of Movie 1 and Movie 2), which assessed that cell orientation was random. The ‘Adhesion/non adhesion assays’ corresponded to substrates with alternated stripes of null and maximum adhesion rate, i.e. to an adhesion contrast of 100% (Fig. 2B, and middle panel of Movie 1 and Movie 2). Cells crossed both stripes types and explored large areas, however their migration was not random. The corresponding rose wind plots were highly anisotropic with an anisotropy index equal to 0.5 for ICAM-1 and VCAM-1, which revealed that lymphocytes were sensitive to the presence of non-adherent zones. Migration of mesenchymal cells are known to be guided by adhesion stripes because they are excluded from non-adherent stripes. Here, lymphocytes were not excluded from non-adherent zones, due their ability to swim over non-adhesive substrates (Aoun et al.). Orientation in adhesion/non-adhesion assays may then result from a difference in speed of leukocytes on adherent and non-adherent zones, which are significant (Aoun et al.), and from other migration bias induced by the contrast of adhesion. However, further investigations on the mechanism would distract us from our main goal. These assays of adhesion/non-adhesion are indeed not informative on adhesive haptotaxis, which refers to guidance on globally adherent substrates. ‘Homogeneous control’ assays and ‘adhesion/non adhesion’ assays are only interesting here as the two extreme controls of actual haptotaxis assays.

Adherent Lymphocytes display haptotaxis by modulations of integrin ligands densities on globally adherent substrates

We then focused on globally adherent substrates, for which alternated stripes were both adherent for lymphocytes, albeit with different adhesion rates. This configuration is reminiscent of blood vessels endothelium, where a minimal adhesion is always required for crawling leukocytes to resist blood flow. The ‘haptotaxis assay’ of Fig. 2C corresponded to alternated stripes with adhesion rates of 0.6 and 0.3, i.e. an adhesion contrast of 50%. The trajectories of cells do not display an obvious directional trend (see also Movie 1 and 2). Some fractions of trajectories followed stripes, whereas others appeared rather perpendicular to stripes. Phenotypes along and across stripes were different from one cell to another and individual cells displayed different phenotypes versus time. Nevertheless, the rose wind plots, corresponding the average of hundreds of cell trajectories, were clearly anisotropic for both ICAM-1 and VCAM-1, with an anisotropy index around 0.4. To ensure that cells adhered on each type of stripe, the adhesion footprint was then probed in situ by reflection interference contrast microscopy (RICM). In Fig. 2D (see also suppl. Mat. Movie 3 and Movie 4), cell body was localized by bright-field images (grey), the distribution of adhesion by fluorescence images of protein A (red) and the footprint of cell adhesion by RICM images (green). Merged images show clearly that cells adhered on both types of stripes. These data confirm unambiguously that the crawling lymphocytes are sensitive to modulations of substrate adhesion on a globally adherent substrate.

Integrin-mediated haptotaxis increases with adhesion contrast

To identify the range of molecular coatings stimulating integrin-mediated haptotaxis, we then varied the adhesion contrast of patterned substrates (Fig. 3). For the haptotaxis assays in which the substrates were globally adhesive, the anisotropy index increased steadily with the adhesion contrast from 0 for an adhesion contrast of 0% to around 0.5 for an adhesion contrast around 55%. For larger adhesion contrasts, data corresponded to ‘adhesion/non adhesion assays’ because the stripes with low molecular density coatings were not adhesive. We previously argued that guidance may result from a crawling bias by non-adherent zones in ‘adhesion/non adhesion assay’, whereas they reveal real haptotaxis sensing phenotype in ‘haptotaxis assay’. However, the data of ‘adhesion/non adhesion assay’ seem to extrapolate the data of ‘haptotaxis assay’ in terms of anisotropy index. At this point, this observation suggests instead that haptotaxis on globally adherent substrates and orientation bias by stripes of null adhesion may result from a similar mechanism and differ only in terms of magnitude.

VLA-4 integrins mediate preference for high adhesion zones

Altogether, the assays with crenel profiles revealed the sensitivity of crawling lymphocytes to modulations of adhesion, i.e. the existence of haptotaxis, but they said nothing about the preferential direction of haptotaxis against a gradient of adhesion. To reveal the preference of cells for more or less adherent zones, we then determined the average distribution of cells on more and less adhesive stripes. In a representative haptotaxis assay on VCAM-1 with adhesion contrast of 40% (Fig. 4A left, middle), a quasi-static state was reached with 60% of cells on more adherent stripes and 40% on less adherent stripes. Importantly, we checked that cells had similar velocities on more or less adhesive stripes (Fig. 4A right). Differential residence time on the different stripes was therefore not due to a difference of speed but to a preference of lymphocytes for higher adhesion zones on VCAM-1. Systematic assays were then performed for different adhesion contrasts, and an index of preferential adhesion, I_{PA} , was calculated as the normalized difference between the numbers of cells on high and low adhesion stripes:

$$\text{Equation 1} \quad I_{PA} = \frac{\# \text{cells on high adhesion} - \# \text{cells on low adhesion}}{\# \text{cells total}}$$

I_{PA} extreme values of 1 and -1 corresponded to cells positioned exclusively on respectively high and low adhesion stripes, whereas a value of 0 corresponded to an equal distribution on both types of stripes. On Fig. 4B, each I_{PA} data point corresponds to the average result from 100 images taken every 10s, each image containing more than 200 cells. I_{PA} increased versus the adhesion contrast from the minimal value 0 (when the difference between stripes vanished) to a maximum value of 0.5. Hence, lymphocytes on VCAM-1 always preferred higher adhesion zones. This tendency resembles the one usually reported in the literature with mesenchymal cells. However, the I_{PA} of mesenchymal cells would be equal to 1 in ‘adhesion/non adhesion’ conditions because they are excluded from non-adherent zones. For lymphocytes, the maximum value reached only 0.6 in ‘adhesion/non adhesion’ conditions because lymphocytes can swim over non-adhesive substrates (Aoun et al.), and are not excluded from non-adherent zones.

LFA-1 integrins mediate unique preference for low adhesion zones

In a representative haptotaxis assay on ICAM-1 at adhesion contrast of 40% (Fig. 4A left and middle), a quasi-static state was reached with 70% of cells on less adherent stripes and 30% on more adherent stripes. Here again, cells velocity was independent of the adhesion contrast of the stripes (Fig. 4A right), so that the unbalance of cell distribution between stripes could not be due to a speed difference. This result indicates therefore a counterintuitive preference of cells for low adhesion zones. Systematic assays confirmed this stunning behavior of ‘reverse haptotaxis’ over a large range of adhesion contrasts (Fig. 4B). I_{PA} started at 0 (when difference between stripes vanished), then decreased versus adhesion contrast to a minimal negative value of -0.35 for an adhesion contrast around 20%, and eventually increased to a plateau value around 0.1 (Fig. 4B). To the best of our knowledge, such a phenotype of adhesive ‘reverse haptotaxis’ has never been observed in the literature. Furthermore, reverse haptotaxis is remarkably sensitive as it appears for adhesion contrasts as low as 10%. In order to rule out possible artifacts due to the patterning method of subtractive printing, we performed similar experiments with substrates obtained by LIMAP additive printing on anti-fouling PEG-coated substrates (Strale et al., 2016). This method has the advantage to avoid any exposure of ICAM-1 proteins to UV/PLPP photo-scission effects. Similar phenotypes of reverse haptotaxis were obtained in the same range of adhesion contrast between 10-50% (Fig. S 1). These results support strongly that ‘reverse haptotaxis’ is not dependent of the patterning method but specifically controlled by LFA-1.

Intracellular calcium signaling is not detected in integrin-mediated haptotaxis

The fact that two different integrins mediate haptotaxis phenotypes with opposite orientations suggests that the mechanism underlying integrin-mediated haptotaxis may use integrins properties beyond their sole adhesion function. At the light of the ICAM-1 results, the hypothesis that guiding on VCAM-1 substrates may simply result from an adhesive bias becomes also more arguable. To shed light on a potential role of integrin-mediated mechanotransduction, we then monitored intracellular calcium activity of lymphocytes crawling on stripe-patterns. Fig. 5 shows that fluctuations in calcium activity for cells crossing stripes of various adhesion remained unaffected on both ICAM-1 and VCAM-1 patterned substrates, whereas control assays with ionomycin showed an instant and intense peak in calcium fluctuations. These data show that intracellular calcium flux is not involved in integrin-mediated haptotaxis. Since calcium signaling is shared by many intracellular signaling pathways (Munaron, 2011), these results challenge a role of mechanotransduction in integrin-mediated haptotaxis of lymphocytes.

Lymphocytes display direct and reverse haptotaxis on gradients of adhesion

All previous experiments were performed with crenel profiles of adhesion to maximize the sensitivity of the detection of haptotaxis. In order to check that lymphocyte haptotaxis also on adhesion gradients with finite steepness, we then patterned substrates with 20 μm wide stripes of low and high adhesion, like in previous experiments, separated by 40 μm wide gradients of increasing and decreasing adhesion (Fig. 6A,B).

Since cells had an average spread diameter of 10-15 μm , they experienced in these assays a gradual change of adhesion in the gradient zones extending over 40 μm . Haptotaxis towards decreasing or increasing gradients eventually lead to cells accumulation in the areas of respectively lower or higher adhesion rate. With a crawling speed of 15 $\mu\text{m}\cdot\text{min}^{-1}$, cells

scanned a gradient zone within a few minutes, so that the transient period between an initially homogeneous distribution of cells (just after sedimentation/adhesion) and a quasi-static distribution of cells after sorting by haptotaxis was short and not easily recorded in experiments. The direction of cell haptotaxis was instead assessed by comparing quasi-static cells distribution (MacNearney et al., 2016) in the areas of lower and upper half sides of adhesion gradients (Fig. 6B). While the analysis of the transient phase can only give access to a limited number of events because it is limited in time, the analysis of the quasi-static regime has no time limit, which allows one to increase statistics just by increasing recording time. On a single representative experiment (Fig. 6C), with 20 gradient stripes and about 200 cells, the distribution of cells was markedly unbalanced in each frame with marked preferences for high adhesion zones on VCAM-1 and low adhesion zones on ICAM-1. These data confirm direct haptotaxis on VCAM-1 and reverse haptotaxis on ICAM-1 with gradient instead of crenels. In order to further probe the robustness of reverse haptotaxis on ICAM-1 for different steepness of gradients, systematic assays were then performed on substrates patterned with saw-tooth profiles and an adhesion contrast of 25% between extrema. Reverse haptotaxis was consistently observed for adhesion gradients extending over 0, 40 and 100 μm (Fig. 7).

Reverse haptotaxis on ICAM-1 gradients is detectable on directed migration of single cells

Observation of single cells directed paths required tracking cells during the transient phase between the initial adhesion of cells and the arrival in their respective accumulation zone (either up or down the gradient depending on their orientation versus a gradient). After this transient phase, cells remained on average in the same preferential accumulation zone due to the on-going guiding effect, so that their average direction was random and directed paths analysis was ill adapted to reveal haptotaxis. The time window to observe directed migration of single haptotaxing cells is therefore limited. This time window could be increased by increasing the spatial width of gradients, but then the gradient slopes and cells directivity would decrease. Linear gradients of width 100 μm were a good compromise because they offered several minutes to observe transient directed path (given the speed of cell of 15 $\mu\text{m}\cdot\text{min}^{-1}$) and haptotaxis is significant (Fig. 7). To grasp the transient regime in its entirety, i.e. the path of each cell from initial adhesion to arrival at the edge of the gradient, we injected cells in the devices at room temperature to keep cells in an inactive and non-adherent state, then temperature was increased 37°C to activate cells. Cells switched one by one to an active state, they acquired a polarized morphology, adhered to the substrate and migrated. Cells were individually tracked for 5 minutes and the few cells reaching the edge of gradients before the end of the 5 mins were rejected from analysis to avoid bias by limit conditions. We prepared ICAM-1 coated substrates with homogeneous adhesion rate of 0.6 as control, and 100 μm wide linear gradients of adhesion rate extrema 0.3 and 0.6. Fig. 8 shows that the directions of cells during the initial 5 minutes of motion were random on a homogeneous substrate along x and y axis, as well as on gradient along y axis. Only directivity along x axis gave a non-null x_{FMI} value of 0.14, which was significant as compared to x_{FMI} of control and to y_{FMI} on gradients. Furthermore, the preferential direction found by directed path on gradient was pointing cells migration towards lower adhesion. These data confirm the existence of reverse haptotaxis mediated by LFA-1, as revealed by the analysis of cells distribution at equilibrium.

DISCUSSION

S.B. Carter (Carter, 1965) defined adhesive haptotaxis in 1965 with cancer cells migrating on cellulose acetate substrates and gradients of palladium. Cells moved in the direction of increasing adhesion and Carter proposed that directed movement was controlled by the relative strength of their peripheral adhesion, hence the name 'haptotaxis' (Greek: haptain, to fasten; taxis, arrangement). Carter foresaw that movement towards surfaces offering greater adhesion could be a general phenomenon applicable to all metazoan cells whose mobility depends on contact with a surface. Indeed, adhesive haptotaxis was later acknowledged for fibroblasts, neurons, stem cells (Amarachintha et al., 2015; Doyle et al., 2009; King et al., 2016; O'Connor et al., 1990; Smith et al., 2004; Thibault et al., 2007), and often attributed to a tug of war between rival parts of the leading edge, those parts that have the strongest grip on the substrate being expected to win (Caballero et al., 2015). Mesenchymal cells are strictly excluded from non-adhesive zones and follow adhesive stripes by default because their motility requires adhesion (Doyle et al., 2009). Similarly, growth cones of neurons also avoid non-adherent substrates (O'Connor et al., 1990). In contrast to these systems, it was recently shown that leukocytes can travel across non-adhesive zones and propel themselves without interaction with a substrate by a motility mode described as swimming (Aoun et al.). Directed motion controlled by adhesion was therefore not conceptually straightforward for leukocytes and its existence remained indeed unproven.

We developed here *in vitro* assays with adhesion patterns characterized by a high spatial resolution (around the micrometer). Repetition of sharp adhesion gradients allowed us to maximize the probability of haptotaxis events, which was instrumental to reveal subtle adhesive haptotaxis phenotype of leukocytes. In these assays, lymphocytes crawled adhesively on patterns with ligands concentration between 200 and 1200 molecules/ μm^2 without change of speed, and that they migrated back and forth between zones of different ligand concentrations. This ubiquitous capacity to explore various adhesive areas *in vitro* may be important for immune cells *in vivo* to achieve an exhaustive spatial survey independently of the adhesion properties of the environment. Nevertheless, our assays showed also that lymphocytes were sensitive to modulations of substrate adhesion, their orientation being significantly biased by adhesive patterns. These results attest that amoeboid cells, here lymphocytes, are capable of adhesive haptotaxis, even if their exploration capacity is barely restricted by adhesion properties.

Efficient guidance by adhesion modulations on globally adhesive substrates is most relevant for leukocytes crawling on blood vessels endothelium because adhesion is required at all times to resist detachment by blood flow. Interestingly, the densities of integrin ligands of 1000 molecules. μm^2 tested in our *in vitro* assays correspond to ICAM-1 and VCAM-1 expression levels found on activated endothelial cells *in vivo* (Dustin and Springer, 1988). These results suggest therefore that integrin-mediated haptotaxis can participate in physiological processes involving spatial modulation of integrin ligands, like transmigration at transmigration cups (Sumagin and Sarelius, 2010), guiding by stromal networks in secondary lymphoid organs (Bajénoff et al., 2006; Hons et al., 2018; Malhotra et al., 2013), or homing to inflamed, wounded or tumoral tissues (Majumdar et al., 2014). In contrast, and according to our results, the idea that lymphocytes could be strictly guided by paths paved with integrin ligands, like trains on a railway, seems invalidated because lymphocytes get easily off-tracks on adhesive patterns *in vitro*. The guidance *in vitro* was nevertheless found sensitive to minute modulations of adhesion with adhesion contrasts as low as 10%. Altogether, our results show that lymphocytes are highly sensitive to subtle modulations of adhesion in a globally adherent

landscape and that the conditions where integrins-mediate haptotaxis is functional exist *in vivo*. There is however no proof yet that adhesive haptotaxis does participate significantly to physiological processes, and this hypothesis will deserve further exploration.

In complete contrast to Carters's foresight that movement towards surfaces offering greater adhesion would be a general phenomenon, lymphocytes with LFA-1 mediated adhesion displayed a marked preference towards surfaces offering lesser adhesion. This unique phenotype of 'reverse haptotaxis' is clearly incompatible with a control by the relative strength of peripheral adhesion, or tug of war mechanism. An alternative mechanism is therefore at work, in which integrins cannot only play a passive role of adhesion linkers. (King et al., 2016) proposed an original mechanism of adhesive haptotaxis for fibroblasts, in which the kinetics of lamellipodia growth was actively regulated by integrins. In this model, engagement of integrins with their ligands promoted activation of Arp2/3 complex and lamellipodial growth (via intermediate activation of FAK, SFK and Rac). This signaling pathway yielded cell reorientation towards higher density of integrin ligands by differential kinetics of lamellipodial growth. This active lamellipodial sensing mechanism proposes an original alternative to the passive tug of war mechanism of Carter. However, it explains cells orientation towards increasing adhesion, and it is therefore not applicable to the reverse haptotaxis of lymphocytes.

Chemotaxis and chemokine-driven haptotaxis are known to rely on signaling pathways that can orient cells towards or against gradients of chemical cue (Amarachintha et al., 2015; Basara et al., 1985; Malet-Engra et al., 2015; Poznansky et al., 2000; Schwarz et al., 2016; Schwarz et al., 2017; Tharp et al., 2006; Weber et al., 2013; Woolf et al., 2007). A tempting hypothesis would be that integrins mechanotransduction may similarly be relayed by specific downstream signaling pathways orienting cells towards or against gradients of adhesion. In support of this hypothesis, the work of Dixit et al (Dixit et al., 2011) defends that integrins mechanotransduction plays a role in the directed migration of neutrophils, and the work of Artemenko et al (Artemenko et al., 2016) supports that mechanical and chemical cues trigger common signaling elements. The hypothesis that mechano- and chemo-taxis share common signaling machineries to orient cells versus an external cue is therefore plausible, and it proposes an elegant explanation for the versatility of cells to orient towards or against a cue gradient. This scenario remains however largely hypothetical because a full link between molecular mechanotransduction and cellular orientation is not deciphered for leukocytes yet. Besides, we addressed here the question of mechano-signaling by monitoring intracellular calcium signaling and found that adhesive haptotaxis of T lymphocytes was not correlated to intracellular calcium signaling. This result is uncommon for cell chemo- and mechano-sensitivity and rather surprising knowing that ion channels usually act as "hubs" in pathways of cell responses to mechanical as well as chemical agonists (Dixit et al., 2011; Lima et al., 2014; Munaron, 2011; Ranade et al., 2015). One option is that haptotaxis involves integrins mechanotransduction with downstream signaling pathways independent of intracellular calcium signaling (Roy et al., 2018). Another option is that mechanotransduction is not involved at all. The question remains open.

Alternatively, a mechanism of versatile adhesive haptotaxis without mechanotransduction could rely on spatio-temporal regulation of integrins affinity states. (Nordenfelt et al., 2016) showed that actin-dependent force appears to regulate integrin activity, and then argue that a coupling between integrin activity and cytoskeletal dynamics could regulate eukaryotic cell orientation, which relaxes the requirement for centralized control of complex pathways. This idea is conceptually rich but it lacks direct evidence at this point. In a related vein, we recently

described a mechanism that explains versatile decisions of lymphocytes to orient with or against a flow in response to the composition of the substrates in integrins ligands ICAM-1 and VCAM-1 (Hornung et al., 2020). Our mechanism relied on the spatial polarization of integrins affinity states along the cell polarization axis, and cross-talk signaling between integrins LFA-1 and VLA-4. Opposite activation of LFA-1 and VLA-4 at cells edges controlled opposite orientations with flow on ICAM-1 and VCAM-1, and an inhibiting crosstalk between integrins triggered a bistable decision of cells between opposite orientations on mixed ICAM-1/VCAM-1 substrates. Complex spatiotemporal regulation of integrins affinity at the cellular scale explained lymphocyte guidance under flow without mechanotransduction. Mechanistic elements of this rheotaxis phenotype may also play a role in adhesive haptotaxis phenotype of lymphocytes. A detailed investigation of integrins activation dynamics in the leading and trailing edges of cells performing haptotaxis would be necessary to shed more light on the interplay between ligand density, integrins affinity distribution, and migration orientation.

In the end, our data revealed that integrins can intervene as efficient and multidirectional guidance mediators, which may intervene in guidance processes of leukocytes and could be inspirational for other cell types guided by integrins such as muscle cells(Chen et al., 2012) or neurons(Huang et al., 2007). Important roles of integrins as adhesive linkers are well identified for leukocytes in the recruitment from blood and lymphatic vessels, where VLA-4 transient adhesion participates to initial rolling, and LFA-1- firm adhesion is required for crawling and diapedesis. These functions concern however leukocyte capture, whereas our work sheds light on leukocyte guidance. Integrins adhesion are also involved in leukocytes trafficking in lymphoid organs and homing to inflamed tissue, however their exact function remains unclear. We show here that integrins cannot promote rigid migration along pathways paved with their ligands because lymphocytes have the ubiquitous ability to explore their environment irrespective of its adhesive properties. At the same time, integrins are efficient multidirectional guidance mediators, and as such, their role might have been underestimated in various processes of leukocyte migration and guiding.

Materials and methods

Cells and reagents

Whole blood from healthy adult donors was obtained from the Etablissement Francais du Sang. Peripheral Blood Mononuclear Cells (PBMC) were recovered from the interface of a Ficoll gradient (Eurobio, Evry, France). T cells were isolated with Pan T cell isolation Kit (Miltenyi Biotec, Bergisch Gladbach, Germany), then activated with antiCD3/antiCD28 Dynabeads (Gibco by Thermo Fischer Scientific, Waltham, MA, USA) according to the manufacturer's instructions. Cells were subsequently cultivated in Roswell Park Memorial Institute Medium (RPMI; Gibco by Thermo Fischer Scientific, Waltham, MA, USA) 1640 supplemented with 25 mM GlutaMax (Gibco by Thermo Fischer Scientific, Waltham, MA, USA), 10% fetal calf serum (FCS; Gibco by Thermo Fischer Scientific, Waltham, MA, USA) at 37°C, 5% CO₂ in the presence of IL-2 (50 ng/ml; Miltenyi Biotec, Bergisch Gladbach, Germany) and used 7 days after activation. At the time of use, the cells were >99% positive for pan-T lymphocyte marker CD3 and assessed for activation and proliferation with CD25, CD45RO, CD45RA and CD69 makers as judged by flow cytometry.

Flow chamber preparation

Glass cover-slips (NEXTERION cover-slip, #1.5H Glass D263, SCHOTT Technical Glass Solutions, Jena, Germany) were first activated by air plasma (Harrick Plasma, Ithaca, NY, USA) for 5 min. Activated glass cover-slips were treated in gas phase with 3-Aminopropyltriethoxysilane (APTS; Sigma-Aldrich, St.Louis, MI) for 1 h and then heated for 15 min at 95°C on a heating plate. Sticky-Slides VI 0.4 (Ibidi GmbH, Martinsried, Germany) were then mounted on treated glass cover-slips. The prepared flow chambers were incubated sequentially at room temperature with an Alexa Fluor™ 647 conjugate Protein A (Thermo Fischer Scientific, Waltham, MA) solution at 50 µg/mL for 1 h, a Bovine Serum Albumin (BSA; Sigma-Aldrich, St.Louis, MI) solution at 4% (w/v) for 15 min, and Fc-ICAM-1 or Fc-VCAM-1 (Intercellular Adhesion Molecule 1; Vascular Cell Adhesion Molecule 1, R&D system, Minneapolis, MN) solution at 10 µg/mL overnight at 4°C. The flow chambers were rinsed extensively with Phosphate Buffered Saline solution (PBS; Gibco by Thermo Fischer Scientific, Waltham, MA) after each incubation.

Photo-patterning of adhesion molecules

We used an inverted microscope (TI Eclipse, Nikon, France) coupled to a UV laser source and a Digital Micromirror Device (Primo™, ALVEOLE, Paris, France) (Strale et al., 2016). Grey level Patterns – either alternated stripes with infinite slope or alternated gradients with finite slope – were projected on ICAM-1 or VCAM-1-treated substrates in presence of a soluble photo-activator (PLPP™, ALVEOLE, Paris, France) to gradually degrade the proteins (Pasturel et al., 2018). Samples were then rinsed with PBS solution and passivated with 4% (w/v) BSA (Sigma-Aldrich, St.Louis, MI) for 15min at room temperature.

Cell adhesion and migration assay

Cell adhesion and migration assays were systematically performed on the same microslide printed for each set of experiment with a homogeneous areas for adhesion assays and patterned areas for migration assays. Cells were seeded into the flow chamber at the concentration of approximately 1.5 million cells/mL and incubated for 10 min at 37°C. Flow of prewarmed and CO₂ equilibrated culture media through the flow chamber was controlled using an Ibidi pump system (Ibidi GmbH, Martinsried, Germany). Cell migration was recorded at 37°C with a Zeiss Z1 automated microscope (Carl Zeiss, Oberkachen, Germany) equipped with a Snap HQ CCD camera (Photometrics, Tucson, AZ), pE-300 white LED microscope illuminator (CoolLED, Andover, UK) and piloted by µManager (Edelstein et al., 2010).

For cell adhesion assay, during each experiment, upon cell seeding and incubation, the flow chamber was then rinsed with culture media with a gentle flow at 1 dyn.cm⁻² to remove non-adherent cells. After rinsing, 100 bright-field images (Plan-Neofluar 10x/0.3 objective, Carl Zeiss, Oberkachen, Germany) were collected every 10 s without flow then under a shear stress at 8 dyn.cm⁻². Fluorescent images for each pattern were collected at the end of the experiment with the same objective at recorded position. The cell adhesion was quantified as the ratio between the number of adherent cells under 8 dyn.cm⁻² and that without flow after rinsing. This ratio is defined as the adhesion rate. For patterns with modulated adhesion, the adhesion contrast is defined as the normalized difference of adhesion rate between areas with maximal adhesion and modulated adhesion.

For cell migration assays, during each experiment, 20 bright-field images (Plan-Neofluar 10x/0.3 objective, Carl Zeiss, Oberkachen, Germany) were first collected every 10s upon incubation to verify the state of the cells. Then, the flow chamber was rinsed with culture

media with a gentle flow of 1 dyn.cm^{-2} to remove non-adherent cells. After rinsing, 100 bright-field images (Plan-Neofluar 10x/0.3 objective, Carl Zeiss, Oberkachen, Germany) were collected every 10s. Fluorescent images for each pattern were collected at the end of the experiment with the same objective and at the same position. Additionally, bright-field and RICM images (Neofluar 63x/1.25 antilex, Carl Zeiss, Oberkachen, Germany) were collected every 5s for each pattern to reveal cell adhesion fingerprint, and fluorescent images were collected at the end of the experiment to localize the protein patterns.

Fluorescent quantification of adhesion molecules

PE-labeled Anti-Human CD54 (ICAM-1) and Anti-Human CD106 (VCAM-1) antibodies (eBioScience by Thermo Fischer Scientific, Waltham, MA, USA) were used for adhesion molecules quantification. First, we set up a bulk calibration curve by measuring the fluorescence intensity of antibody solutions inside thin channels of $48 \mu\text{m}$ in height at concentrations of 0, 1.5, 3, 5 and $7 \mu\text{g/mL}$. Channels were pre-treated with 1% Pluronic F127[®] (Sigma-Aldrich, St Louis, MO) to limit adsorption of antibodies on channel surface. In the end, channels were rinsed extensively with PBS. Residual fluorescent intensity due to adsorbed antibodies was measured and then subtracted from the previous measurements. Previous study (Hornung et al.) showed a linear relation between the fluorescent intensity and the bulk concentration. We assume that the signal is given by the total number of molecules in the thin channel, then the volume concentration can be converted to a surface concentration for a channel of $48 \mu\text{m}$ in height. Then, for each sample used for cell adhesion and migration assay, the patterned surfaces coated with ICAM-1 or VCAM-1 were first rinsed extensively with cold PBS solution. Then, the sample was stained with corresponding antibody at $10 \mu\text{g/mL}$ and incubated overnight at 4°C . Images were taken the next day with the Zeiss Z1 microscope set-up. The fluorescent intensity was analyzed with ImageJ software (U. S. National Institutes of Health, Bethesda, USA) at 5 different positions. The average intensity was converted into surface density of the adhesion molecules according the calibration data.

Cell tracking and data analysis

A home-made program developed with MATLAB software (The MathWorks, Natick, MA) was used to track migrating cells as previously described in (Valignat et al., 2013). Briefly, the program 1) performs image quality enhancement using background division and intensity normalization; 2) binarizes the images using a given threshold to distinguish cells from the background; 3) detects and numbers cells in the first frame and tracks them in the following frames; 4) saves the coordinates and time points for each identified cell to calculate different migration parameters. Only cells migrating for at least $30 \mu\text{m}$ were considered. In this study, to quantify cell adhesion, the program counted the number of adherent cells at 0 dyn.cm^{-2} and 8 dyn.cm^{-2} to determine the adhesion rate of patterned substrates. To determine the directional bias of migrating cells on patterned surface, the migration angle was defined as the one between the patterned stripes and the total cell trajectory between the first and final image. The program calculated the fraction of cells with a migration angle $<45^\circ$ and $>45^\circ$. The anisotropy index was defined as the difference between these two fractions. To further characterize the preference of cells on patterns with modulated adhesion, the program used a binarized image of the fluorescent pattern as a mask to identify the position of each cell on the pattern. It then displayed color-coded cell trajectories according to their position on the patterns. It also calculated the number of cells on patterns with higher and lower adhesion.

The Index of Preferential Adhesion was defined as the normalized difference of these two numbers.

Fluorescent detection of Calcium Flux

For calcium flux imaging experiments, cells were first seeded in channels with RPMI medium and were incubated for 10 min at 37°C to allow adhesion, then they were rinsed with HBSS + 1% BSA and incubated with Oregon Green[®] 488 BAPTA-1, AM (ThermoFisher, Waltham, USA) diluted in HBSS + 1% BSA to a concentration of 5 µM for 15 min at 37°C in the dark. After rinsing with HBSS + 1% BSA, the medium was replaced by HBSS+ 10% FCS. Control experiment was achieved by injection ionomycin (ThermoFisher, Waltham, USA) at a concentration of 1 µg.mL⁻¹. The calcium intensity fluctuation for each migrating cell was calculated for the whole duration of experiment as such: first, the minimal fluorescent intensity for the first twenty images was calculated. Then, the fluorescent fluctuation was calculated as the normalized different between the intensity of the migrating cell and the minimal intensity. Finally, the average fluctuation for all migrating cells was generated for the whole duration of experiment. Then, the average fluctuation for all migrating cells was generated for the whole duration of experiment.

Conflict of interests

Vincent Studer is a shareholder of Alvéole. Pierre-Olivier Strale is an employee of Alvéole.

Author Contributions

XL and VSDN performed all experiments and analysis. XL, LA, OT, VS and POS developed printing protocols. MBP managed the control of cells culture and characterizations. MPV developed analysis protocols, and participated in experiments, analysis and project design. OT designed the project, supervised experiments and analysis, and wrote the paper.

Acknowledgements:

This work was supported by Agence Nationale de la Recherche (RECRUTE - ANR-15-CE15-0022; ILIAAD ANR-18-CE09-0029), LABEX INFORM, Région Sud, Turing Centre for Living systems for financial support, and Excellence Initiative of Aix-Marseille University –A*MIDEX, a French “Investissements d’Avenir” programme. We are also grateful to the Cell Culture Platform facility (Luminy TPR2-INSERM).

List of Figures

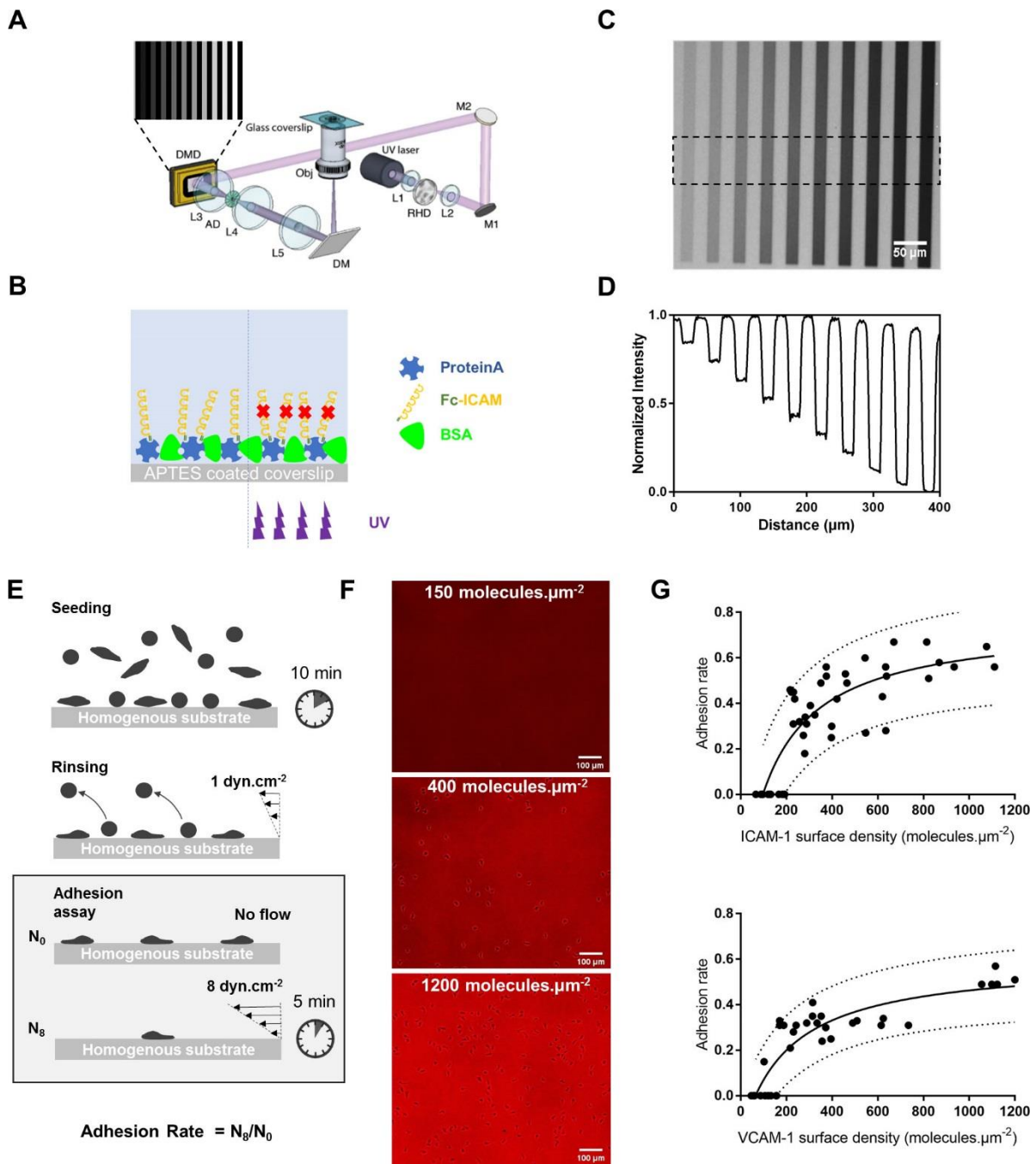


Fig. 1: Optical patterning yields substrates with various amounts of grafted integrins ligands and with modulated adhesion. (A) Illustration of the optical set-up used for protein patterning (Strale et al., 2016). (B) Illustration of the experimental protocol for ICAM-1 patterning on glass coverslips. Substrates were functionalized with APTES, coated with fluorescent protein A, passivated with BSA, incubated with Fc-ICAM-1 or Fc-VCAM-1, and finally UV-illuminated in presence of photoinitiator PLPP to modulate the amount of functional integrin ligands. (C) Image of fluorescent Protein A obtained after optical patterning with stripes corresponding to 10, 20, 30, 40, 50, 60, 70, 80, 90 and 100% of a maximal dose of $800 \text{ mJ} \cdot \text{mm}^{-2}$. (D) Profile of fluorescence intensity corresponding to image (C) after background correction and normalization. (E) Illustration of cell adhesion assay: after 10 min incubation, cells were rinsed with a gentle flow of $1 \text{ dyn} \cdot \text{cm}^{-2}$ to remove non adherent cells. After this initial washing, the number of adherent cells was quantified without flow (N_0) and with a flow of $8 \text{ dyn} \cdot \text{cm}^{-2}$ (N_8). The adhesion rate was defined as the ratio between N_8 and N_0 . (F) Merge of fluorescence images (red) and

transmission images (grey) showing fluorescent Protein A and lymphocytes adherent on ICAM-1 substrates. Quantification of ICAM-1 yielded densities of 150 molecules. μm^{-2} (top), 400 molecules. μm^{-2} (middle) and 1200 molecules. μm^{-2} (bottom). **(G)** Adhesion rate versus ICAM-1 (top) and VCAM-1 (bottom) surface density. A Langmuir fit was used as a guide for the eye with a confidence interval of 90% indicated by the black dashed curves.

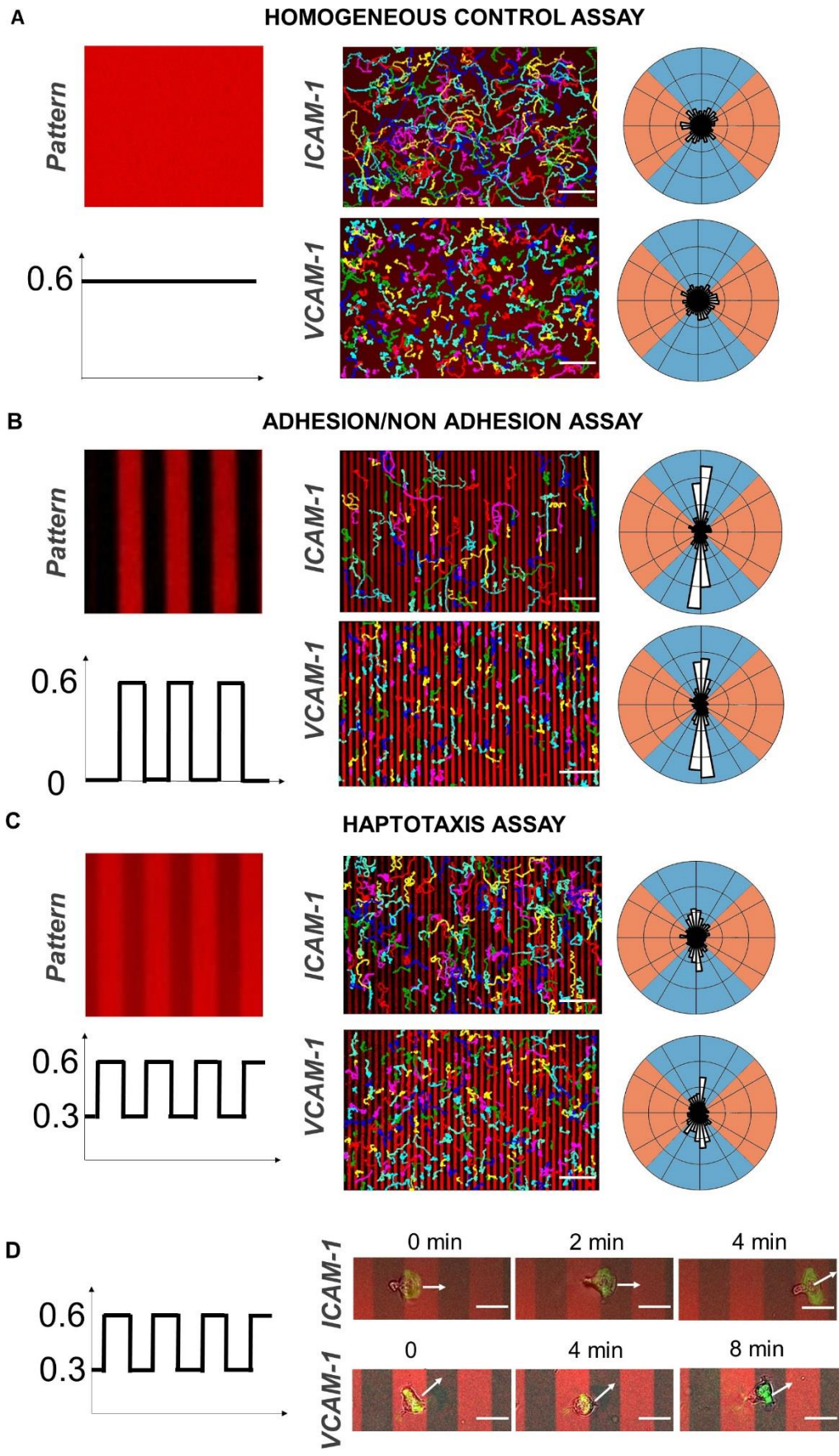


Fig. 2: Adherent Lymphocytes display haptotaxis versus modulations of integrin ligand density. (Left) Fluorescent image of protein A patterns (top) and illustration of the corresponding adhesion profiles

(bottom). **(Middle)** Merge images of cell trajectories and of protein A patterns for ICAM-1 (top) and VCAM-1 (bottom) coated substrates in a representative experiment. **(Right)** Histogram showing the angular distribution of the trajectories taking into account the first and last points of each trajectory for a representative experiment on ICAM-1 (top) and VCAM-1 (bottom) substrates. **(A)** 'Homogenous control assay' on substrates with homogeneous coatings. Cells migrated in random directions, anisotropy index was null. **(B)** 'Adhesion/non-adhesion assay' on substrates with alternated stripes of maximum and null adhesion. Cells direction was biased in the vertical quadrants, anisotropy index was 0.5. **(C)** 'Haptotaxis assay' on substrates of alternated adhesive stripes with adhesion rate 0.6 and 0.3. Cell direction was biased in the vertical quadrants, anisotropy index was 0.4. In rose wind plots, bins correspond to 10° , external circle to 15% and colors indicate vertical (blue) and horizontal (red) quadrants for anisotropy index calculation. Displayed trajectories correspond to one representative experiment and cell number of 195 and 343 cells in (A), 100 and 253 cells in (B) and 189 and 313 cells in (C) for ICAM-1 and VCAM-1 substrates respectively. Rose wind plots correspond to 5 independent experiments (Cell number 1090 and 1081 cells in (A), 256 and 641 cells in (B), and 256 and 641 cells in (C), for ICAM-1 and VCAM-1 substrates respectively). Scale bar=200 μm . **(D)** RICM microscopy reveals global cell adhesion in 'haptotaxis assays'. Merge images of bright-field images (grey), RICM images of adhesion footprint (green), and fluorescent images of protein A (red). White arrows indicate the direction of cell migration. Adhesion signal (green) is detected on both stripes with high and low adhesion rates. Scale bar=20 μm

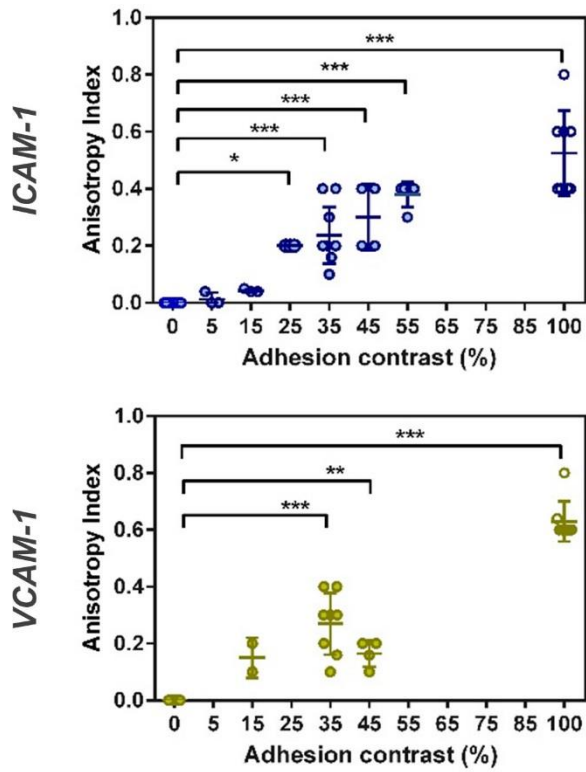


Fig. 3 : **Integrin-mediated haptotaxis increases with adhesion contrast.** Anisotropy index versus adhesion contrast of ICAM-1 (blue) and VCAM-1 (green) substrates. Each data point corresponds to the average anisotropy index calculated for one experiment comprising 100 images taken every 10s with $N_{\text{cells}} > 200$ per experiment. Error bars are standard deviations for independent experiments. * $P < 0.05$, ** $P < 0.001$, *** $P < 0.0001$ with respect to homogeneous substrate, one-way ANOVA followed by the Tukey multiple comparison test.

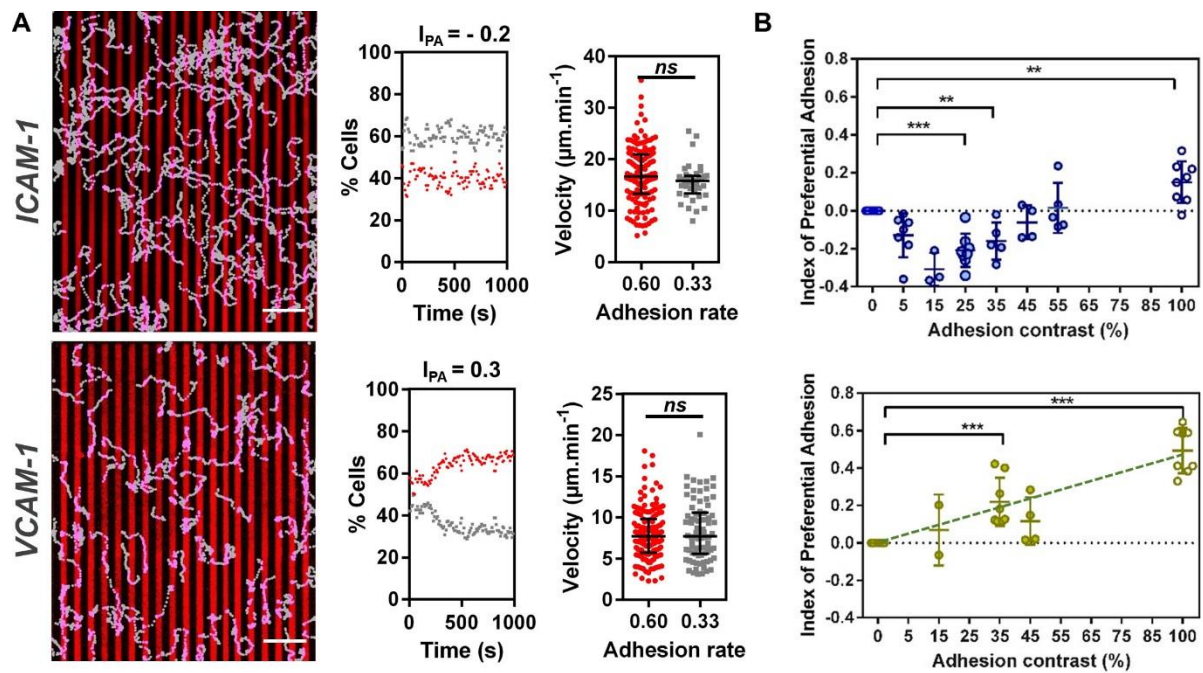


Fig. 4: Integrin mediated haptotaxis prefers lower adhesion zone with ICAM-1 and higher adhesion zone with VCAM-1. (A) Representative experiment of haptotaxis with an adhesion contrast 40 % on ICAM-1 (top) and VCAM-1 (bottom). **Left-** Cell trajectories on more adhesive (pink) and less adhesive (grey) stripes. Scale bar=200µm. **Middle-** Percentage of cells versus time on more adhesive (red) and less adhesive (grey) stripes. **Right-** Average velocity of individual cells plotted for cells migrating on more adhesive (red) and less adhesive (grey) coatings. Statistical analysis with unpaired t test revealed no statistical significance between two groups of data. (B) Index of preferential adhesion I_{PA} versus adhesion contrast of ICAM-1 (blue) and VCAM-1 (green). Each data point corresponds to the average I_{PA} calculated for one experiment of 100 images taken every 10s and $N_{cells} > 200$ per experiment.. Error bars are standard deviations for independent experiments. Green dotted line correspond to linear regression with $R=0.92$. * $P < 0.05$, ** $P < 0.001$, *** $P < 0.0001$ with respect to homogeneous substrate, one way ANOVA followed by the Tukey multiple comparison test.

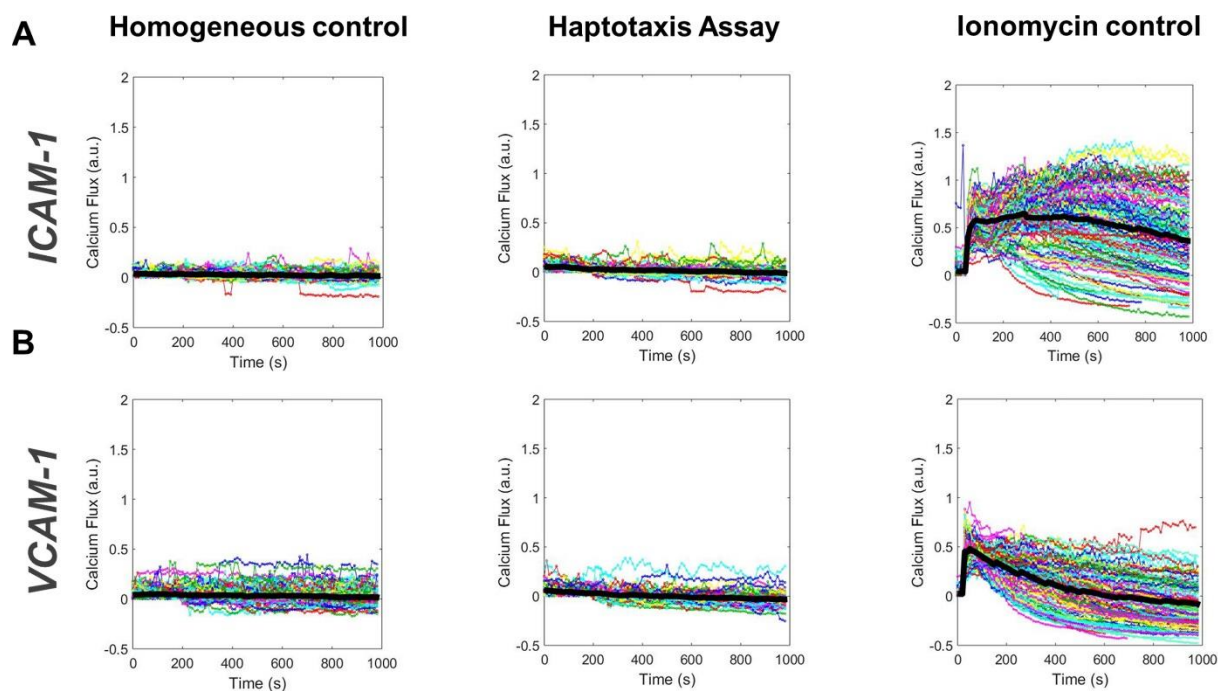


Fig. 5 : Intercellular Calcium flux detection shows no evidence of mechanotransduction in integrin-mediated haptotaxis. The normalized calcium signaling intensity I_N was calculated for each cell and each frame as $I_N = (I - I_{min}) / I_{min}$, where I and I_{min} are respectively the instant and minimal calcium signaling for each cell. Each colored line represents one migrating cell and the thick black line corresponds to the average value for all cells. Normalized calcium signaling versus time on cells migrating on ICAM-1 (**A**) and VCAM-1 (**B**) substrates. For homogenous (**left**) and haptotaxis assay (**middle**), no intercellular Calcium flux was detected, whereas the control experiment with ionomycin (**right**) revealed an instant strong signal.

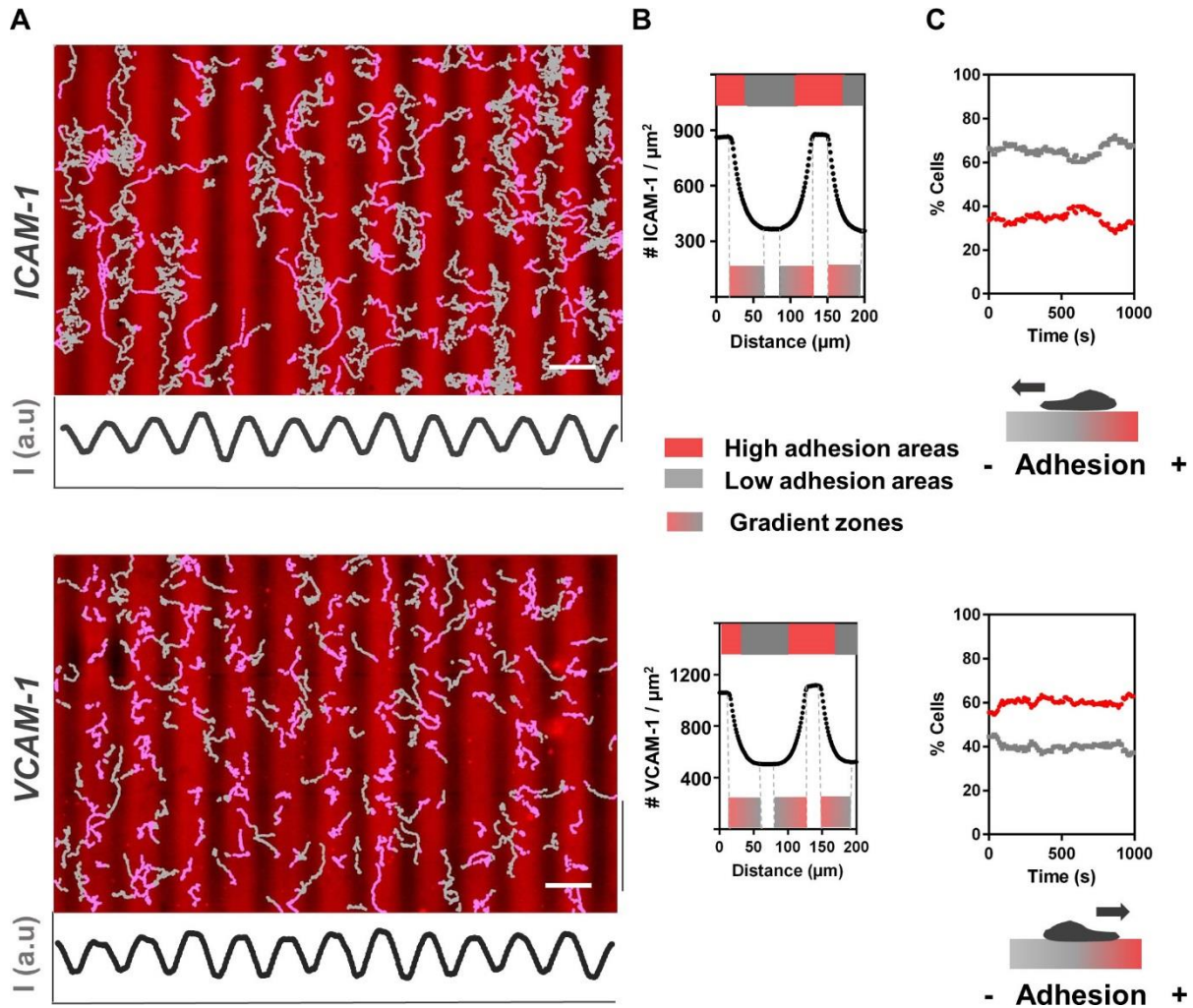


Fig. 6 : lymphocytes orient either with adhesion gradients on VCAM-1 and against adhesion gradients on ICAM-1. (A) Cells trajectories in a representative experiment on substrates patterned by ICAM-1 (top) and VCAM-1 (bottom) with $20\ \mu\text{m}$ wide stripes of high (red) and low (grey) adhesion separated by ascending and descending gradients extending over $40\ \mu\text{m}$. The profile below images correspond to the profile of fluorescent protein A. Pink and grey trajectories indicate cell tracks over high and low adhesion areas, respectively. Scale bar = $200\ \mu\text{m}$ (B) Quantitative profiles of CAM concentration in molecules per μm^2 . The high and low adhesion areas used to count cells preferential positioning are indicated respectively by the red and grey bars. The bars with color gradients illustrate the position and direction of the adhesion gradients. (C) Percentage of cells on high (red) and low (grey) adhesion areas plotted versus time. Each data point corresponds to one frame of the time lapse of the representative experiments in A, with 178 and 217 cells per frame for respectively ICAM-1 and VCAM-1 experiments. The data show systematic preference for low and high adhesion areas on respectively ICAM-1 and VCAM-1, which is illustrated by cartoons of reverse haptotaxis on ICAM-1 and direct haptotaxis on VCAM-1.

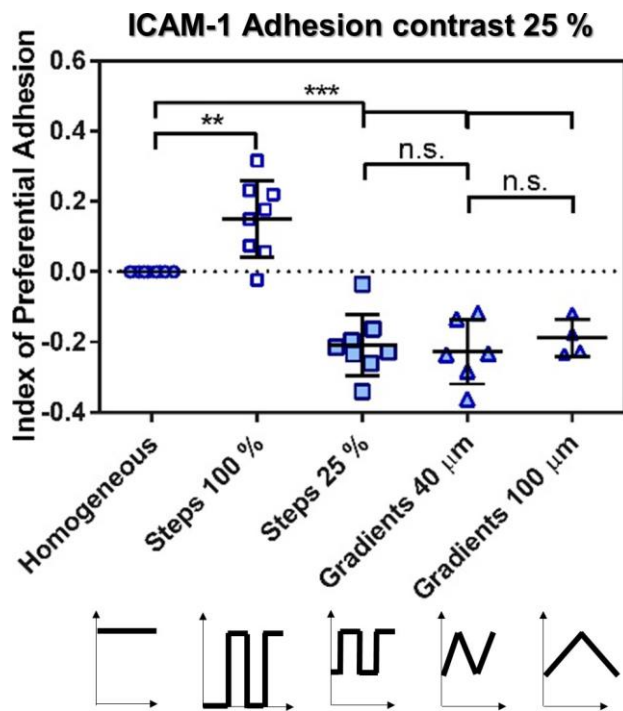


Fig. 7: **Reverse haptotaxis on ICAM-1 exists for different steepness of gradients.** IPA for homogeneous substrates (round dots), for adhesion/non adhesion assay or steps with 100% adhesion contrast (hollow square dots), and for haptotaxis assays with constant adhesion contrast of 25% and varying steepness of gradients (filled dots). Gradients extensions are ranging between 0 μm with crenels profiles (filled square dots), and 40 to 100 μm with saw tooth profiles (Filled triangle dots). Each data point corresponds to the average IPA calculated for one experiment of 100 images taken every 10s, and Ncells > 200 per experiment. Error bars are standard deviations for independent experiments. * $P < 0.05$, ** $P < 0.001$, *** $P < 0.0001$, one way ANOVA followed by the Tukey multiple comparison test.

SUPPLEMENTARY MATERIALS

Preference for lower adhesion on ICAM-1 substrates patterned by additive printing

In order to verify that haptotaxis phenotypes do not rely on artefactual effects due to the innovative subtractive printing protocol, we also performed migration experiments on patterns similar to the ones of Fig. 4 but obtained by additive LIMAP printing (Strale et al., 2016). Migration results displayed the same trends with additive and subtractive printing with a marked preferential residence on lower adhesion patterns in a wide range of adhesion contrasts below 55%. Subtractive printing was however favored for systematic experimentations because we had a slightly lesser fraction of non-motile cells on additive printed substrates. In the additive printed experiments, glass cover-slips (NEXTERION cover-slip, #1.5H Glass D263, SCHOTT Technical Glass Solutions, Jena, Germany) were first activated by air plasma (Harrick Plasma, Ithaca, NY, USA) for 5 min, then treated for 2 h in liquid phase with 3-Aminopropyltriethoxysilane (APTS; Sigma-Aldrich, St.Louis, MI) diluted at 1% in water with 0.03% Acid acetic and heated for 15 min at 95°C on a heating plate. Sticky-Slides VI 0.4 (Ibidi GmbH, Martinsried, Germany) were then mounted on treated glass cover-slips. The prepared flow chambers were incubated at 4°C overnight with of 0,23 g.ml⁻¹ PEG-SVA (mPEG-SVA MW: 5000Da; Interchim) solution with NaHCO₃ at 10 mM, then rinsed with milliQ water, incubated with 4% (w/v) BSA (Sigma-Aldrich, St.Louis, MI) for 15min at room temperature and rinsed with Phosphate Buffered Saline solution (PBS; Gibco by Thermo Fischer Scientific, Waltham, MA). Grey level patterns were then projected on substrates in presence of photo-activator (PLPP™, ALVEOLE, Paris, France) to locally activate the substrate (Strale et al., 2016). Samples were then incubated with an Alexa Fluor™ 647 conjugate Protein A (Thermo Fischer Scientific, Waltham, MA) solution at 50 µg/mL for 1 h, a Bovine Serum Albumin (BSA; Sigma-

Aldrich, St.Louis, MI) solution at 4% (w/v) for 15 min, and Fc-ICAM-1 (Intercellular Adhesion Molecule 1, R&D system, Minneapolis, MN) solution at 10 $\mu\text{g}/\text{mL}$ overnight at 4°C. The flow chambers were finally rinsed extensively with Phosphate Buffered Saline solution (PBS; Gibco by Thermo Fischer Scientific, Waltham, MA) after each incubation.

The index of preferential migration followed similar trend in the full range of adhesion contrast whether substrates were prepared by additive (Fig. S1) or subtractive (Fig. 4) printing.

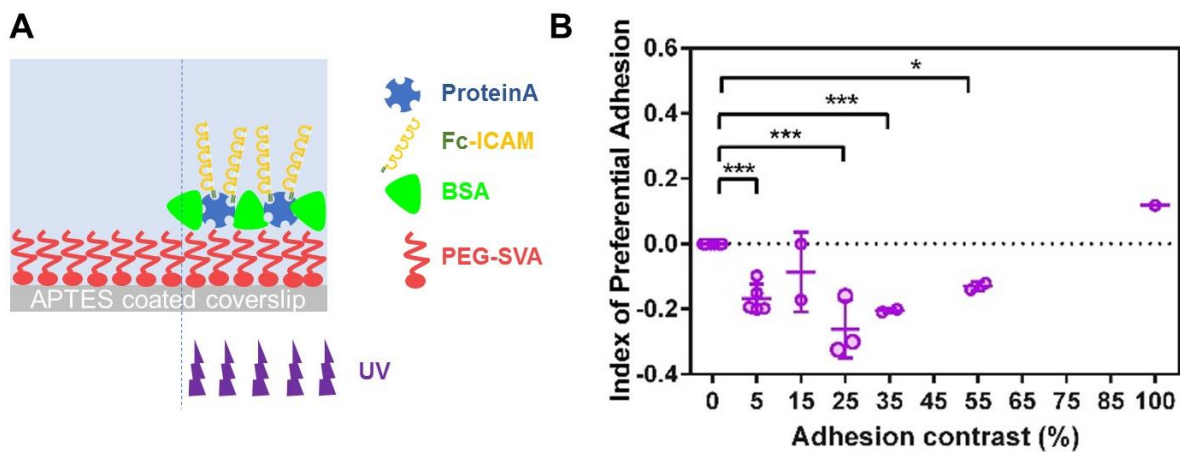


Fig. S 1 (A) Illustration of the experimental protocol for ICAM-1 additive patterning on glass coverslips. Substrates were functionalized with APTES and PEG-SVA, UV-illuminated in presence of photoinitiator PLPP, and finally incubated with fluorescent protein A, passivated with BSA, and incubated with Fc-ICAM-1 (B) Index of preferential adhesion I_{PA} versus adhesion contrast of ICAM-1 (blue) on stripe patterns similar as for Fig. 4 but prepared by LIMAP additive printing. Each data point corresponds to the average IPA calculated for one experiment by pooling 100 images taken every 10s. Error bars are standard deviations for different experiments. Ncells > 200 per data point.

Analysis of single cell directed migration during transient segregation along a gradient provides less statistics than analysis of cell population distribution along gradient at equilibrium

While directed migration of single cells during transient travel along a gradient could reveal haptotaxis (Fig. 8), Fig. S 2 shows that the corresponding raw trajectories were only faintly biased by the gradient. Tracks overlaid over the origin were distributed almost equally between opposite directions. This faint haptotaxis response to adhesion cues is consistent with the fact that lymphocytes migration depends hardly on the substrate adhesion properties and that lymphocytes have the exceptional ability to travel back and forth across adherent and non-adherent patterns (Fig. 2,3 and Aoun et al 2019). The study of adhesive haptotaxis requires therefore large statistics to extract clear tendencies with lymphocytes, and the

analysis of single cell directed migration during transient segregation is therefore not the most appropriated approach. The time window during which cells travels along the gradient is indeed limited, and the duration of transient segregation is shorter for higher gradient slopes and more pronounced haptotaxis . In contrast, analysis of cell population distribution has no time limit in a given experiment, so that high statistics and clear tendencies are easily accessible by increasing the recording time in each given experiment, and this approach is appropriate for any gradient slope. These advantages were implemental to study lymphocyte adhesive haptotaxis and allow us to scrutinize systematically and finely various conditions of adhesion contrasts and gradients slopes.

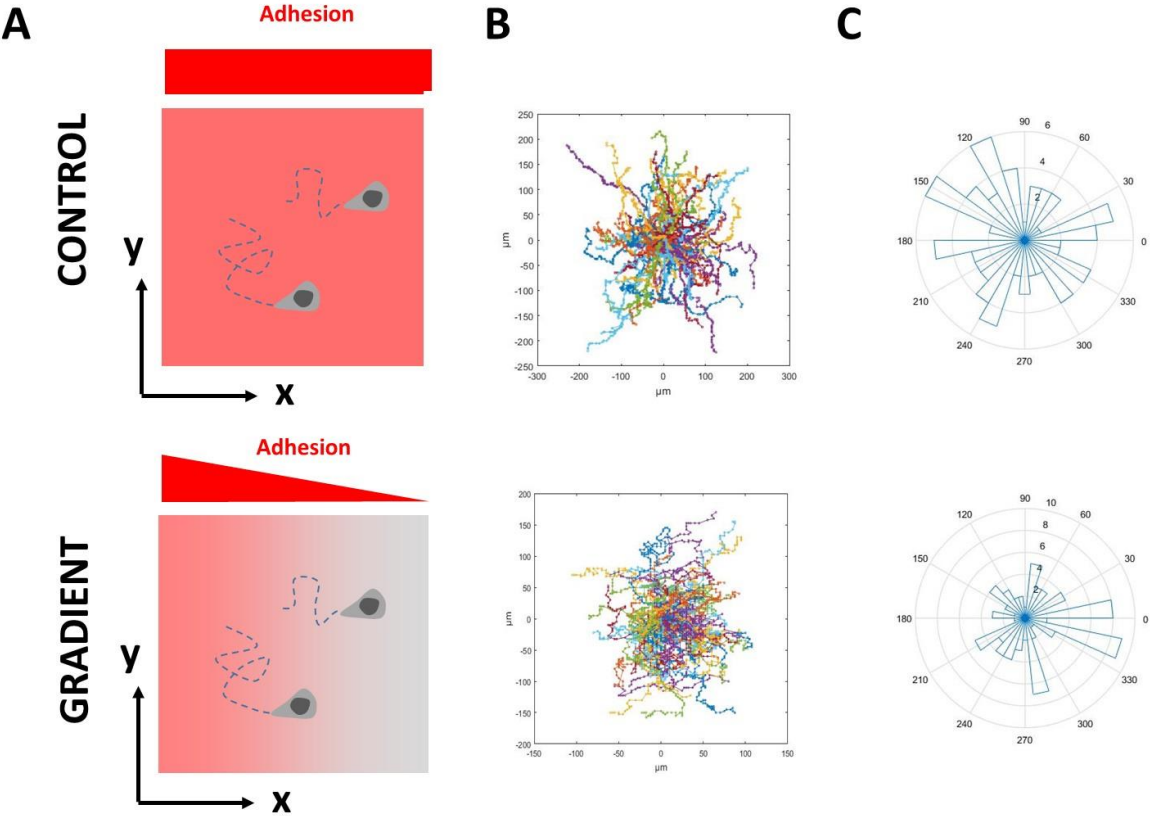


Fig. S 2: Directed paths are hardly pronounced for adhesion haptotaxis of lymphocytes even in optimum conditions of observation. A- Cartoon illustrating cells migration on homogeneous substrates (Top) and on a gradient of adhesion increasing along the x axis homogenous along the y axis (Bottom). B- Tracks of individual cells overlaid on the origin. C- Roseplot histograms of the angles formed by the starting point and position after 5 min of migration with the x-axis.

Supplementary Movies

Movie 1: T cell haptotactic migration on patterned ICAM-1 substrates. Left: negative control substrate with 0% adhesion contrast; Middle: positive control substrate with 100% adhesion contrast; Right: substrate with 50% adhesion contrast. In red: substrate with higher adhesion; In grey: bright-field images of migrating cells. Scale bar=50 μ m

Movie 2: T cell haptotactic migration on patterned VCAM-1 substrates. Left: negative control substrate with 0% adhesion contrast; Middle: positive control substrate with 100% adhesion contrast; Right: substrate with 50% adhesion contrast. In red: substrate with higher adhesion; In grey: bright-field images of migrating cells. Scale bar=50 μ m

Movie 3: RICM movies of T cells haptotaxis assay on patterned ICAM-1 substrates. In green: cell adhesion patch shown by RICM; In red: patterned stripes with modulated ligand density; In grey: bright-field images showing cell body. Scale bar=20 μ m

Movie 4: RICM movies of T cells haptotaxis assay on patterned VCAM-1 substrates. In green: cell adhesion patch shown by RICM; In red: patterned stripes with modulated ligand density; In grey: bright-field images showing cell body. Scale bar=20 μ m

Bibliography

- Amarachintha, S. P., Ryan, K. J., Cayer, M., Boudreau, N. S., Johnson, N. M. and Heckman, C. A.** (2015). Effect of Cdc42 domains on filopodia sensing, cell orientation, and haptotaxis. *Cell. Signal.* **27**, 683–693.
- Aoun, L., Negre, P., Farutin, A., Garcia-Seyda, N., Rivzi, M. S., Galland, R., Michelot, A., Luo, X., Biarnes-Pelicot, M., Hivroz, C., et al.** Mammalian Amoeboid Swimming is propelled by molecular and not protrusion-based paddling in Lymphocytes. *BioRxiv MS ID BIORXIV2018509182*.
- Artemenko, Y., Axiotakis, L., Borleis, J., Iglesias, P. A. and Devreotes, P. N.** (2016). Chemical and mechanical stimuli act on common signal transduction and cytoskeletal networks. *Proc. Natl. Acad. Sci.* **113**, E7500–E7509.
- Aznavoorian, S., Stracke, M. L., Krutzsch, H., Schiffmann, E. and Liotta, L. A.** (1990). Signal Transduction for Chemotaxis and Haptotaxis by Matrix Molecules in Tumor Cells. *The Journal of Cell Biology* **110**, 1427–1438.
- Bajénoff, M., Egen, J. G., Koo, L. Y., Laugier, J. P., Brau, F., Glaichenhaus, N. and Germain, R. N.** (2006). Stromal Cell Networks Regulate Lymphocyte Entry, Migration, and Territoriality in Lymph Nodes. *Immunity* **25**, 989–1001.
- Basara, M. L., McCarthy, J. B., Barnes, D. W. and Furcht, L. T.** (1985). Stimulation of Haptotaxis and Migration of Tumor Cells by Serum Spreading Factor. *Cancer Res.* **45**, 2487–2494.
- Berry, M. F., Engler, A. J., Woo, Y. J., Pirolli, T. J., Bish, L. T., Jayasankar, V., Morine, K. J., Gardner, T. J., Discher, D. E. and Sweeney, H. L.** (2006). Mesenchymal stem cell injection after myocardial infarction improves myocardial compliance. *Am. J. Physiol.-Heart Circ. Physiol.* **290**, H2196–H2203.
- Brandley, B. K. and Schnaar, R. L.** (1989). Tumor cell haptotaxis on covalently immobilized linear and exponential gradients of a cell adhesion peptide. *Dev. Biol.* **135**, 74–86.
- Burger, J. A., Ghia, P., Rosenwald, A. and Caligaris-Cappio, F.** (2009). The microenvironment in mature B-cell malignancies: a target for new treatment strategies. *Blood* **114**, 3367–3375.
- Caballero, D., Comelles, J., Piel, M., Voituriez, R. and Riveline, D.** (2015). Ratchetaxis: Long-Range Directed Cell Migration by Local Cues. *Trends Cell Biol.* **25**, 815–827.
- Canton, B.** (2008). Refinement and standardization of synthetic biological parts and devices. *Nat Biotechnol* **26**, 787–793.
- Carman, C. V. and Springer, T. A.** (2004). A transmigratory cup in leukocyte diapedesis both through individual vascular endothelial cells and between them. *J. Cell Biol.* **167**, 377–88.

- Carter, S.** (1965). Principles of cell motility: the direction of cell movement and cancer invasion. *Nature* **208**, 1183.
- Carter, S. B.** (1967). Haptotaxis and the Mechanism of Cell Motility. *Nature* **213**, 256–260.
- Chen, X., Su, Y.-D., Ajeti, V., Chen, S.-J. and Campagnola, P. J.** (2012). Cell Adhesion on Micro-Structured Fibronectin Gradients Fabricated by Multiphoton Excited Photochemistry. *Cell. Mol. Bioeng.* **5**, 307–319.
- Dixit, N., Yamayoshi, I., Nazarian, A. and Simon, S. I.** (2011). Migrational Guidance of Neutrophils Is Mechanotransduced via High-Affinity LFA-1 and Calcium Flux. *J. Immunol.* **187**, 472–481.
- Dominguez, G. A., Anderson, N. R. and Hammer, D. A.** (2015). The direction of migration of T-lymphocytes under flow depends upon which adhesion receptors are engaged. *Integr Biol* **7**, 345–355.
- Doyle, A. D., Wang, F. W., Matsumoto, K. and Yamada, K. M.** (2009). One-dimensional topography underlies three-dimensional fibrillar cell migration. *J. Cell Biol.* **184**, 481–490.
- Dustin, M. L. and Springer, T. A.** (1988). Lymphocyte function-associated antigen-1 (LFA-1) interaction with intercellular adhesion molecule-1 (ICAM-1) is one of at least three mechanisms for lymphocyte adhesion to cultured endothelial cells. *J. Cell Biol.* **107**, 321 LP – 331.
- Edelstein, A., Amodaj, N., Hoover, K., Vale, R. and Stuurman, N.** (2010). Computer Control of Microscopes Using μ Manager. In *Current Protocols in Molecular Biology*, pp. 14.20.1-14.20.17. Hoboken, NJ, USA: John Wiley & Sons, Inc.
- Gattei, V., Bulian, P., Principe, M. I. D., Zucchetto, A., Maurillo, L., Buccisano, F., Bomben, R., Dal-Bo, M., Luciano, F., Rossi, F. M., et al.** (2008). Relevance of CD49d protein expression as overall survival and progressive disease prognosticator in chronic lymphocytic leukemia. *Blood* **111**, 865–873.
- Gorina, R., Lyck, R., Vestweber, D. and Engelhardt, B.** (2014). beta(2) Integrin-Mediated Crawling on Endothelial ICAM-1 and ICAM-2 Is a Prerequisite for Transcellular Neutrophil Diapedesis across the Inflamed Blood-Brain Barrier. *J. Immunol.* **192**, 324–337.
- Granger, D. and Kubes, P.** (1994). The Microcirculation and Inflammation - Modulation of Leukocyte-Endothelial Cell-Adhesion. *J. Leukoc. Biol.* **55**, 662–675.
- Hons, M., Kopf, A., Hauschild, R., Leithner, A., Gaertner, F., Abe, J., Renkawitz, J., Stein, J. V. and Sixt, M.** (2018). Chemokines and integrins independently tune actin flow and substrate friction during intranodal migration of T cells. *Nat. Immunol.* **19**, 606–616.

- Hornung, A., Sbarrato, T., Garcia-Seyda, N., Aoun, L., Luo, X., Biarnes-Pelicot, M., Theodoly, O. and Valignat, M.-P.** (2020). A Bistable Mechanism Mediated by Integrins Controls Mechanotaxis of Leukocytes. *Biophys. J.* **118**, 565–577.
- Hornung, A., Sbarrato, T., Garcia-Seyda, N., Aoun, L., Luo, X., Biarnes-Pelicot, M., Theodoly, O. and Valignat, M.-P.** A Bistable Mechanism Mediated by Integrins Controls Mechanotaxis of Leukocytes. *BioRxiv ID BIORXIV2018509091ID*.
- Huang, Z., Yazdani, U., Thompson-Peer, K. L., Kolodkin, A. L. and Terman, J. R.** (2007). Crk-associated substrate (Cas) signaling protein functions with integrins to specify axon guidance during development. *Development* **134**, 2337–2347.
- King, S. J., Asokan, S. B., Haynes, E. M., Zimmerman, S. P., Rotty, J. D., Alb, J. G., Tagliatela, A., Blake, D. R., Lebedeva, I. P., Marston, D., et al.** (2016). Lamellipodia are crucial for haptotactic sensing and response. *J Cell Sci* **129**, 2329–2342.
- Klominek, J., Robert, K.-H. and Sundqvist, K.-C.** (1993). Chemotaxis and Haptotaxis of Human Malignant Mesothelioma Cells: Effects of Fibronectin, Laminin, Type IV Collagen, and an Autocrine Motility Factor-like Substance¹. *Cancer Research* **53**, 4376–4382.
- Lämmermann, T., Bader, B. L., Monkley, S. J., Worbs, T., Wedlich-Söldner, R., Hirsch, K., Keller, M., Förster, R., Critchley, D. R., Fässler, R., et al.** (2008a). Rapid leukocyte migration by integrin-independent flowing and squeezing. *Nature* **453**, 51–55.
- Lämmermann, T., Bader, B. L., Monkley, S. J., Worbs, T., Wedlich-Söldner, R., Hirsch, K., Keller, M., Förster, R., Critchley, D. R., Fässler, R., et al.** (2008b). Rapid leukocyte migration by integrin-independent flowing and squeezing. *Nature* **453**, 51–55.
- Lämmermann, T., Afonso, P. V., Angermann, B. R., Wang, J. M., Kastenmüller, W., Parent, C. A. and Germain, R. N.** (2013). Neutrophil swarms require LTB₄ and integrins at sites of cell death in vivo. *Nature* **498**, 371–375.
- Lima, W. C., Vinet, A., Pieters, J. and Cosson, P.** (2014). Role of PKD2 in Rheotaxis in Dictyostelium. *PLOS ONE* **9**, e88682.
- Liu, X., Ma, B., Malik, A. B., Tang, H., Yang, T., Sun, B., Wang, G., Minshall, R. D., Li, Y., Zhao, Y., et al.** (2012). Bidirectional regulation of neutrophil migration by mitogen-activated protein kinases. *Nat. Immunol.* **13**, 457.
- MacNearney, D., Mak, B., Ongo, G., Kennedy, T. E. and Juncker, D.** (2016). Nanocontact Printing of Proteins on Physiologically Soft Substrates to Study Cell Haptotaxis. *Langmuir* **32**, 13525–13533.
- Majumdar, R., Sixt, M. and Parent, C. A.** (2014). New paradigms in the establishment and maintenance of gradients during directed cell migration. *Curr. Opin. Cell Biol.* **30**, 33–40.
- Malawista, S. E., de Boisfleury Chevance, A. and Boxer, L. A.** (2000). Random locomotion and chemotaxis of human blood polymorphonuclear leukocytes from a patient with

- Leukocyte Adhesion Deficiency-1: Normal displacement in close quarters via chimneying. *Cytoskeleton* **46**, 183–189.
- Malet-Engra, G., Yu, W., Oldani, A., Rey-Barroso, J., Gov, N. S., Scita, G. and Dupré, L.** (2015). Collective Cell Motility Promotes Chemotactic Prowess and Resistance to Chemorepulsion. *Curr. Biol.* **25**, 242–250.
- Malhotra, D., Fletcher, A. L. and Turley, S. J.** (2013). Stromal and hematopoietic cells in secondary lymphoid organs: partners in immunity. *Immunol. Rev.* **251**, 160–176.
- Massena, S. and Phillipson, M.** (2012). Intravascular Leukocyte Chemotaxis: The Rules of Attraction. In *Hematology - Science and Practice* (ed. Lawrie, C.), p. InTech.
- Mccarthy, J. B. and Furcht, L. T.** (1984). Laminin and Fibronectin Promote the Haptotactic Migration of B16 Mouse Melanoma Cells In Vitro. *The Journal of Cell Biology* **98**, 1474–1480.
- Motta, C. M. M., Endres, K. J., Wesdemiotis, C., Willits, R. K. and Becker, M. L.** (2019). Enhancing Schwann cell migration using concentration gradients of laminin-derived peptides. *Biomaterials* **218**, 119335.
- Munaron, L.** (2011). Shuffling the cards in signal transduction: Calcium, arachidonic acid and mechanosensitivity. *World J. Biol. Chem.* **2**, 59–66.
- Nordenfelt, P., Elliott, H. L. and Springer, T. A.** (2016). Coordinated integrin activation by actin-dependent force during T-cell migration. *Nat. Commun.* **7**, 13119.
- O'Connor, T. P., Duerr, J. S. and Bentley, D.** (1990). Pioneer growth cone steering decisions mediated by single filopodial contacts in situ. *J. Neurosci.* **10**, 3935–3946.
- Oudin, M. J., Miller, M. A., Klazen, J. A. Z., Kosciuk, T., Lussiez, A., Hughes, S. K., Tadros, J., Bear, J. E., Lauffenburger, D. A. and Gertler, F. B.** (2016). MenalNV mediates synergistic cross-talk between signaling pathways driving chemotaxis and haptotaxis. *Mol. Biol. Cell* **27**, 3085–3094.
- Overstreet, M. G., Gaylo, A., Angermann, B. R., Hughson, A., Hyun, Y.-M., Lambert, K., Acharya, M., Billroth-MacLurg, A. C., Rosenberg, A. F., Topham, D. J., et al.** (2013). Inflammation-induced interstitial migration of effector CD4⁺ T cells is dependent on integrin α V. *Nat. Immunol.* **14**, 949–958.
- Paluch, E. K., Aspalter, I. M. and Sixt, M.** (2016). Focal Adhesion–Independent Cell Migration. *Annu. Rev. Cell Dev. Biol.* **32**, 469–490.
- Park, E. J., Peixoto, A., Imai, Y., Goodarzi, A., Cheng, G., Carman, C. V., Andrian, U. H. von and Shimaoka, M.** (2010). Distinct roles for LFA-1 affinity regulation during T-cell adhesion, diapedesis, and interstitial migration in lymph nodes. *Blood* **115**, 1572–1581.
- Pasturel, A., Strale, P.-O. and Studer, V.** (2018). A generic widefield topographical and chemical photopatterning method for hydrogels.

- Poznansky, M. C., Olszak, I. T., Foxall, R., Evans, R. H., Luster, A. D. and Scadden, D. T.** (2000). Active movement of T cells away from a chemokine. *Nat. Med.* **6**, 543–548.
- Ranade, S. S., Syeda, R. and Patapoutian, A.** (2015). Mechanically Activated Ion Channels. *Neuron* **87**, 1162–1179.
- Ricoult, S. G., Kennedy, T. E. and Juncker, D.** (2015). Substrate-bound protein gradients to study haptotaxis. *Front. Bioeng. Biotechnol.* **3**, 1–12.
- Ross, T. D., Coon, B. G., Yun, S., Baeyens, N., Tanaka, K., Ouyang, M. and Schwartz, M. A.** (2013). Integrins in mechanotransduction. *Curr. Opin. Cell Biol.* **25**, 613–618.
- Roy, J., Mazzaferri, J., Filep, J. G. and Costantino, S.** (2017). A Haptotaxis Assay for Neutrophils using Optical Patterning and a High-content Approach. *Sci. Rep.* **7**,.
- Roy, N. H., MacKay, J. L., Robertson, T. F., Hammer, D. A. and Burkhardt, J. K.** (2018). Crk adaptor proteins mediate actin-dependent T cell migration and mechanosensing induced by the integrin LFA-1. *Sci. Signal.* **11**,.
- Schwarz, J., Bierbaum, V., Merrin, J., Frank, T., Hauschild, R., Bollenbach, T., Tay, S., Sixt, M. and Mehling, M.** (2016). A microfluidic device for measuring cell migration towards substrate-bound and soluble chemokine gradients OPEN. *Nat. Publ. Group.*
- Schwarz, J., Bierbaum, V., Vaahtomeri, K., Hauschild, R., Brown, M., de Vries, I., Leithner, A., Reversat, A., Merrin, J., Tarrant, T., et al.** (2017). Dendritic Cells Interpret Haptotactic Chemokine Gradients in a Manner Governed by Signal-to-Noise Ratio and Dependent on GRK6. *Curr. Biol.* **27**, 1314–1325.
- Smith, J. T., Tomfohr, J. K., Wells, M. C., Beebe, T. P., Kepler, T. B. and Reichert, W. M.** (2004). Measurement of Cell Migration on Surface-Bound Fibronectin Gradients. *Langmuir* **20**, 8279–8286.
- Smith, L. A., Aranda-Espinoza, H., Haun, J. B., Dembo, M. and Hammer, D. A.** (2007). Neutrophil Traction Stresses are Concentrated in the Uropod during Migration. *Biophys. J.* **92**, L58–L60.
- Strale, P.-O., Azioune, A., Bugnicourt, G., Lecomte, Y., Chahid, M. and Studer, V.** (2016). Multiprotein Printing by Light-Induced Molecular Adsorption. *Adv. Mater.* **28**, 2024–+.
- Sullivan, K. E., Quinn, K. P., Tang, K. M., Georgakoudi, I. and Black, L. D.** (2014). Extracellular matrix remodeling following myocardial infarction influences the therapeutic potential of mesenchymal stem cells. *Stem Cell Res. Ther.* **5**, 14.
- Sumagin, R. and Sarelius, I. H.** (2010). Intercellular Adhesion Molecule-1 Enrichment near Tricellular Endothelial Junctions Is Preferentially Associated with Leukocyte Transmigration and Signals for Reorganization of These Junctions To Accommodate Leukocyte Passage. *J. Immunol.* **184**, 5242–5252.

- Sumagin, R., Prizant, H., Lomakina, E., Waugh, R. E. and Sarelius, I. H.** (2010). LFA-1 and Mac-1 Define Characteristically Different Intraluminal Crawling and Emigration Patterns for Monocytes and Neutrophils In Situ. *J. Immunol.* **185**, 7057–7066.
- Tharp, W. G., Yadav, R., Irimia, D., Upadhyaya, A., Samadani, A., Hurtado, O., Liu, S.-Y., Munisamy, S., Brainard, D. M., Mahon, M. J., et al.** (2006). Neutrophil chemorepulsion in defined interleukin-8 gradients in vitro and in vivo. *J. Leukoc. Biol.* **79**, 539–554.
- Thibault, M. M., Hoemann, C. D. and Buschmann, M. D.** (2007). Fibronectin, Vitronectin, and Collagen I Induce Chemotaxis and Haptotaxis of Human and Rabbit Mesenchymal Stem Cells in a Standardized Transmembrane Assay. *Stem Cells Dev.* **16**, 489–502.
- Valignat, M. P., Theodoly, O., Gucciardi, A., Hogg, N. and Lellouch, A. C.** (2013). T lymphocytes orient against the direction of fluid flow during LFA-1-mediated migration. *Biophys. J.* **104**, 322–331.
- Valignat, M.-P., Nègre, P., Cadra, S., Lellouch, A. C., Gallet, F., Hénon, S. and Theodoly, O.** (2014). Lymphocytes can self-steer passively with wind vane uropods. *Nat. Commun.* **5**, 5213.
- van Gils, J. M., Ramkhalawon, B., Fernandes, L., Stewart, M. C., Guo, L., Seibert, T., Menezes, G. B., Cara, D. C., Chow, C., Kinane, T. B., et al.** (2013). Endothelial Expression of Guidance Cues in Vessel Wall Homeostasis: Dysregulation under pro-atherosclerotic conditions. *Arterioscler. Thromb. Vasc. Biol.* **33**, 911–919.
- Weber, M., Hauschild, R., Schwarz, J., Moussion, C., Vries, I. de, Legler, D. F., Luther, S. A., Bollenbach, T. and Sixt, M.** (2013). Interstitial Dendritic Cell Guidance by Haptotactic Chemokine Gradients. *Science* **339**, 328–332.
- Wen, J. H., Choi, O., Taylor-Weiner, H., Fuhrmann, A., Karpiak, J. V., Almutairi, A. and Engler, A. J.** (2015). Haptotaxis is cell type specific and limited by substrate adhesiveness. *Cell. Mol. Bioeng.* **8**, 530–542.
- Woolf, E., Grigorova, I., Sagiv, A., Grabovsky, V., Feigelson, S. W., Shulman, Z., Hartmann, T., Sixt, M., Cyster, J. G. and Alon, R.** (2007). Lymph node chemokines promote sustained T lymphocyte motility without triggering stable integrin adhesiveness in the absence of shear forces. *Nat. Immunol.* **8**, 1076–1085.
- Wu, C., Asokan, S. B., Berginski, M. E., Haynes, E. M., Sharpless, N. E., Griffith, J. D., Gomez, S. M. and Bear, J. E.** (2012). Arp2/3 is critical for lamellipodia and response to extracellular matrix cues but is dispensable for chemotaxis. *Cell* **148**, 973–987.
- Zaidel-Bar, R., Kam, Z. and Geiger, B.** (2005). Polarized downregulation of the paxillin-p130CAS-Rac1 pathway induced by shear flow. *J. Cell Sci.* **118**, 3997–4007.